THESIS FOR THE DEGREE OF DOCTOR OF PHILOSOPHY

Mixed Oxide Oxygen Carriers for Chemical-Looping Combustion

PETER K. HALLBERG

Department of Space, Earth and Environment

CHALMERS UNIVERSITY OF TECHNOLOGY

Gothenburg, Sweden 2017

Mixed Oxide Oxygen Carriers for Chemical-Looping Combustion
PETER HALLBERG
ISBN 978-91-7597-604-4

Doktorsavhandlingar vid Chalmers tekniska högskola
Ny serie nr 4285
ISSN 0346-718X

Department of Space, Earth and Environment
Chalmers University of Technology
SE-412 96 Gothenburg
Sweden
Telephone + 46 (0)31-772 1000

Printed at Chalmers Reproservice AB
Gothenburg, Sweden 2017

Mixed Oxide Oxygen Carriers for Chemical-Looping Combustion
PETER HALLBERG
Department of Space, Earth and Environment
Chalmers University of Technology

ABSTRACT

Chemical-Looping Combustion is a promising method for combustion with inherent carbon dioxide capture. Oxygen is provided to the fuel with a solid oxygen carrier. The oxygen carrier is circulated between the reactor for fuel oxidation and another reactor where it is reoxidized with air. A good performing oxygen carrier is vital for this process. An oxygen carrier is typically a metal oxide and this work focus on evaluating oxygen carriers based on mixed metal oxides.

A method was developed to determine the reduction reaction enthalpy of oxygen carriers in a fluidized-bed batch reactor. The method was verified using a nickel based oxygen carries with known enthalpy. Different oxygen carriers based of the iron-titanium oxide ilmenite were evaluated to determine the reaction enthalpy in a chemical-looping process.

Oxygen carriers manufactured with spray drying technology were developed through a screening process. Starting with 79 different materials those deemed promising were tested in a fluidized-bed batch reactor. The ability to release oxygen, reactivity with fuel and fluidization behavior were the most important parameters and based off the results 10 materials were chosen to be investigated in a small continuous Chemical-Looping reactor system. Based off these results 2 materials were examined in a larger continuous Chemical-Looping reactor system where fuel power up to 6 kW were used.

Oxygen carrier particles based on calcium manganite performed best with substantial release off oxygen and high to complete conversion on fuel. The material $CaMn_{0.775}Ti_{0.125}Mg_{0.1}O_{3-\delta}$ performed best in all three reactor systems. In addition to the oxygen release and reactivity these particles also proved durable with unaffected reactivity and low attrition after 99 h of continuous chemical-looping operation.

Keywords: Chemical-Looping Combustion (CLC), Chemical-Looping with oxygen uncoupling, oxygen carrier, ilmenite, calcium manganite, CO_2 capture

LIST OF PUBLICATIONS

This thesis is based on the work contained in the following papers:

Paper I
Hallberg, P.; Leion H.; Lyngfelt, A., A Method for determination of reaction enthalpy of oxygen carriers for chemical looping combustion – Application to ilmenite. *Thermochimica Acta* **2011**, 524, 62-67

Paper II
Hallberg, P.; Jing, D.; Rydén, M.; Mattisson, T.; Lyngfelt, A., Chemical Looping Combustion and Chemical Looping with Oxygen Uncoupling Experiments in a Batch Reactor Using Spray-Dried $CaMn_{1-x}M_xO_{3-\delta}$ (M = Ti, Fe, Mg) Particles as Oxygen carriers. *Energy & Fuels* **2013**, 27, 1473-1481

Paper III
Hallberg, P.; Källén, M.; Jing, D.; Snijkers, F.; van Noyen, J.; Rydén, M.; Lyngfelt, A., Experimental Investigation of $CaMnO_{3-\delta}$ Based Oxygen Carriers Used in Continuous Chemical-Looping Combustion. *International Journal of Chemical Engineering*, **2014**, Article ID 412517, 9 pages

Paper IV
Hallberg, P.; Hanning, M.; Rydén, M.; Mattisson, T.; Lyngfelt, A., Investigation of a calcium manganite as oxygen carrier during 99 h of operation of chemical-looping combustion in a 10 kW_{th} reactor unit. *International Journal of Greenhouse Gas Control* **2016**, 53, 222-229

Paper V
Källén, M.; Hallberg, P.; Rydén, M.; Mattisson, T.; Lyngfelt, A.; Combined Oxides of Iron, Manganese and Silica as Oxygen Carriers for Chemical-Looping Combustion. *Fuel processing technology* **2014**, 124, (August 2014), 87-96.

Contribution report
Principal author, responsible for the experimental work and data evaluation in paper I.
Principal author, responsible for data evaluation and part of the experimental work paper II.
Principal author, responsible for part of data evaluation and part of the experimental work paper III.
Principal author, shared responsibility for experimental work and data evaluation in paper IV.
Shared responsibility for writing, experimental work and data evaluation in paper V.

RELATED PAPERS NOT INCLUDED IN THE THESIS

- Schwebel, G.; Hallberg, P.; Krumm, W., Leion, H., Kinetic description derived from fluidized bed experiments for ilmenite as oxygen carrier in chemical-looping combustion. *Proceedings of the 36th International Technical Conference on Clean Coal and Fuel Systems* **2011**.
- Jing, D. ; Mattisson, T. ; Rydén, M.; Hallberg, P.; Hedayati, A.; van Noyen, J.; Snijkers, F.; Lyngfelt, A., Innovative Oxygen Carrier Materials for Chemical-Looping Combustion, *Energy Procedia: International Conference on Greenhouse Gas Technologies (GHGT)* **2013,** 37, 645-653.
- Hallberg, P.; Rydén, M.; Mattisson, T., Lyngfelt, A., CaMnO3-δ Made from Low Cost Material Examined as Oxygen Carrier in Chemical-looping Combustion. *Energy Procedia: 12th International Conference on Greenhouse Gas Control Technologies, Austin*, October 2014. 63, 80-86
- Jing, D.; Snijkers, F.; Hallberg, P.; Leion, H.; Mattisson, T.; Lyngfelt, A., Effect of Production Parameters on the Spray-Dried Calcium Manganite Oxygen Carriers for Chemical-Looping Combustion. *Energy & Fuels* **2016**, 30 (4), 3257-3268
- Schmitz, M.; Linderholm, C. ; Hallberg, P.; Sundqvist, S. E.; Lyngfelt, A., Chemical-Looping Combustion of Solid Fuels using Manganese Ores as Oxygen Carriers. *Energy & Fuels **2016***, 30, 1204–1216

CONTENTS

ACKNOWLEDGEMENTS

I like to thank the people that have contributed in making this thesis happen.

My main supervisor Anders Lyngfelt with his invaluable experience and tireless attitude.

My co-supervisor Magnus Rydén for encouraging discussions.

Henrik Leion for friendly guiding me into the field.

Tobias Mattisson for good advice and useful tips.

My friends and colleagues in the CLC-group always generous with time and help: Patrick, Jesper, Dazheng, Malin, Mattias, Golnar, Sebastian, Calle, Ulf, Georg, Mehdi, Ali, Erik, Volkmar, Pavleta.

The A-team who makes everything work smoothly.

The other colleagues at Energy Technology and Inorganic Environmental Chemistry for the friendly atmosphere and funny lunch discussion.

European taxpayers who through the European Commission financed the projects.

My friends who help me take my mind off work.

My wife for always being there and the best team mate I could wish for.

/Peter

Mixed-Oxide Oxygen Carriers for Chemical-Looping Combustion

1. INTRODUCTION

1.1 Global warming

For over 100 years it has been known that carbon dioxide in the atmosphere traps heat[1]. Some of the radiation from the sun is absorbed by earth's surface and converted to heat. The heat causes infrared radiation which is absorbed and reemitted by greenhouse gases in the atmosphere increasing the temperature of earth's surface. Since the start of industrialization the atmospheric concentration of carbon dioxide and other greenhouse gases have increased. Most of the increase of carbon dioxide is due to combustion of fossil fuel[2].

The atmospheric concentration of carbon dioxide has surpassed 400 ppm and is steadily increasing with a present rate of over 2 ppm per year. To limit future disastrous effects of global warning the trend of increasing emissions need to be reversed. Limiting the emissions will however be difficult since around 86 % of the world primary energy is fossil and infrastructure is built long term.

1.2 Carbon dioxide Capture and Storage/Sequestration (CCS)

There are different options to decrease carbon dioxide emissions and many of them will be needed to have a chance to reach climate goals[3]. One option is to capture carbon dioxide from large emission sources and subsequently transport it to locations where it will not reach the atmosphere. Figure 1.2.1Figure 1.2.1 is from the IPCC Special Report on Carbon Dioxide Capture and Storage and presents an overview of the entire CCS chain. Examples of large emission sources are power plants, refineries and industry, for example steel and cement production. The carbon dioxide would be separated, compressed and then transported by pipeline or ship to a storage site. Storage sites could be depleted gas or oil reservoirs or deep saline aquifers. The carbon dioxide can also be used for enhanced oil recovery. While this would not eliminate carbon dioxide emission it would be a substantial reduction compared to conventionally produced oil. Generally the geological storage consists of a porous layer, where the carbon dioxide are injected, covered by a nonporous cap rock. Another alternative is mineralization where the carbon dioxide reacts with certain metal oxides present in common rocks to produce solid carbonates. An example of carbon dioxide capture and storage together with enhanced oil recovery is a project in Boundary Dam in Canada where carbon dioxide is separated from a power plant by amine absorption and sold to be used for enhanced oil recovery at Weyburn Oil Field [4].

There are different methods to separate carbon dioxide in combustion processes. All of them require energy for the separation process and thus lowering the efficiency of the overall process. One method is post-combustion capture where there is a conventional combustion and the carbon dioxide is separated from the flue gas. Similar technology is used in the natural gas processing industry. Post-combustion separation include amine absorption processes. An advantage of post-combustion separation is that it is possible to use for retrofit of existing units, not only power plants but also industrial processes such as cement production and refineries. In pre-combustion separation gasification at high pressure is followed by water-gas-shift and thereafter separation of carbon dioxide and hydrogen. The technology is used in fertilizer and hydrogen production. In oxyfuel combustion there is first an energy requiring air separation step to get a pure oxygen stream. The fuel is burnt with oxygen together with recycled flue gases to be able to keep the boiler at an acceptable temperature for the boiler tubing because pure oxygen would result in a higher boiler temperature. [5]

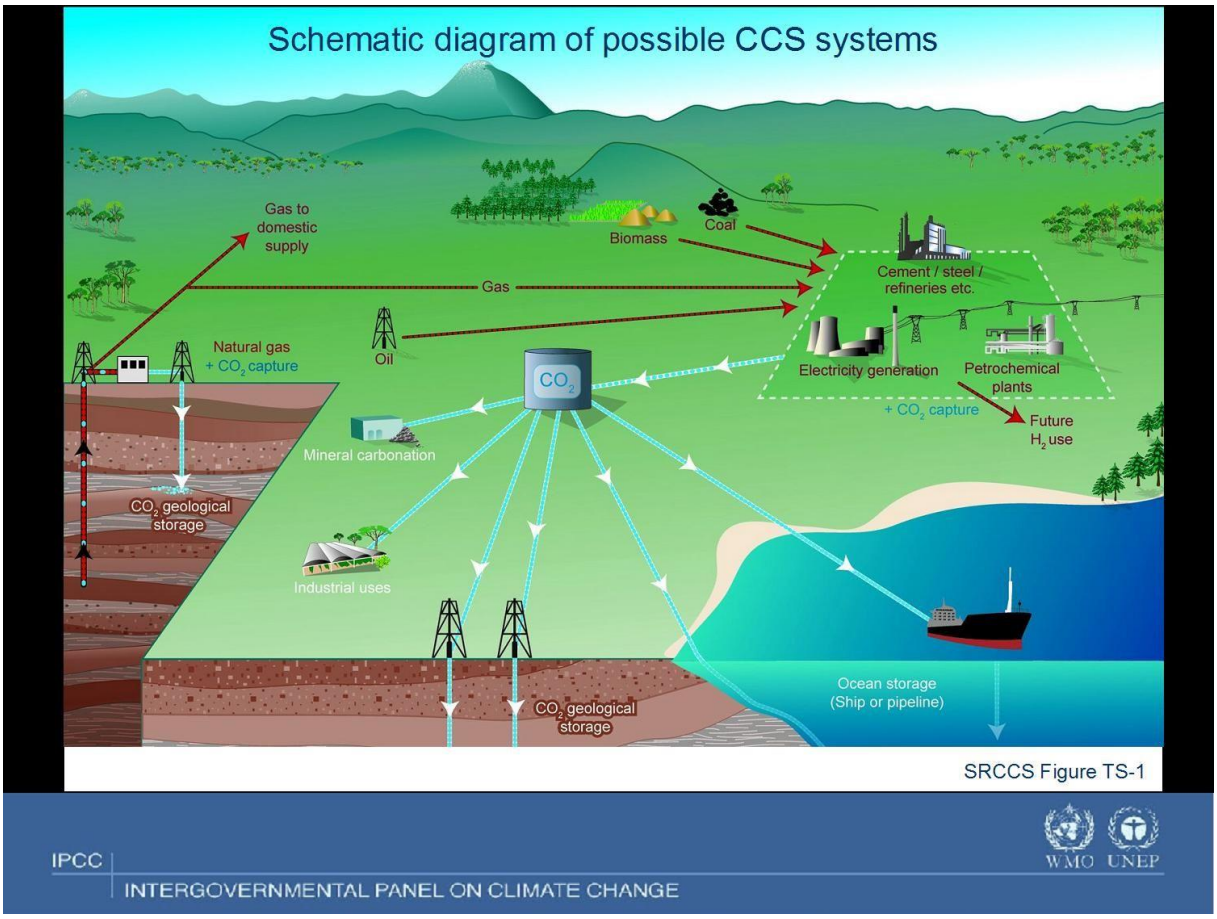

Figure 1.2.1 Schematic image of possible CCS systems showing the sources for which CCS might be relevant, transport of CO2 and storage options. From IPPC Special Report on Carbon Dioxide Capture and Storage [5].

1.3 Chemical-looping Combustion (CLC)

Chemical-looping combustion is a fuel oxidation process with inherent CO_2 separation[6]. In CLC oxygen is provided to the fuel with a solid oxygen carrier, which is usually a metal oxide. Systems where the oxygen carrier is continuously circulated between two reactors has been successfully tested in different scales. A schematic image of the general process is shown in Figure 1.3.1.

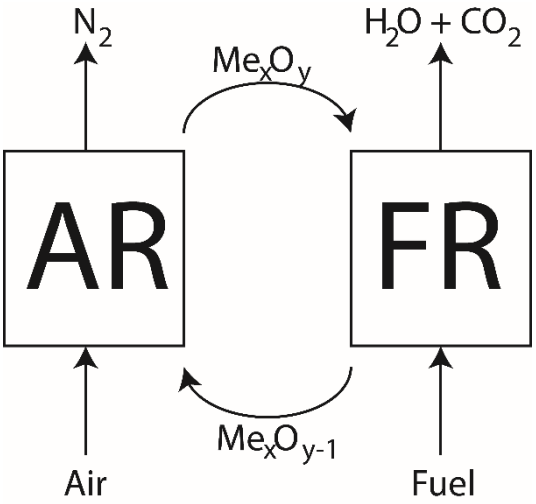

Figure 1.3.1 A schematic image of the Chemical-looping Combustion process.

In the fuel reactor (FR) the fuel is oxidized by the oxygen carrier, denoted Me_xO_y, according to reaction (1). The flue gases consist of mainly CO_2 and steam. Steam is easily condensed so that almost pure CO_2

remains. So by preventing dilution of the flue gases with nitrogen from the air, ideally no energy consuming gas separation is needed to obtain CO_2 of sufficiently high purity for transport and storage. This makes CLC an almost ideal technology for CCS. Another important advantage over conventional combustion is that due to the relatively low temperature used, typically around 1000 °C, thermal NO_X formation is avoided. Moreover, fuel NO_X is limited to the fuel reactor which could be beneficial for separation compared to conventional combustion. After the fuel oxidation, the oxygen depleted oxygen carrier is transferred to the air reactor (AR) to be reoxidized with air according to reaction (2). Note that the sum of reaction (1) and (2) is identical to conventional combustion and thus the heat output from CLC is the same as conventional combustion.

$$C_nH_{2m} + (2n+m)Me_xO_y \rightarrow nCO_2 + mH_2O + (2n+m)Me_xO_{y-1} \quad (1)$$

$$O_2 + 2Me_xO_{y-1} \rightarrow 2Me_xO_y \quad (2)$$

Reaction (1) is typically considered as a gas-solid reaction. So when the fuel is a solid, such as coal or biomass char, an intermediate step is needed where the char is gasified. This can be done according to reaction (3) or reaction (4) using steam or carbon dioxide as reagent.

$$C + CO_2 \rightarrow 2CO \quad (3)$$

$$C + H_2O \rightarrow H_2 + CO \quad (4)$$

The most common way of achieving a suitable reactor for creating contact between the solid oxygen carrier and the reacting gas is by fluidization. Fluidization is a process where a solid, granular material is made to behave like a fluid by passing gas up through the solid, a basic diagram of the process is shown in Figure 1.3.2. With sufficient gas velocity the upward drag force will counteract the gravitational pull. Thus, it is possible to circulate the particles from one reactor to another. Circulating fluidized beds are used in commercial scale in for example conventional boilers so the technology is well established.

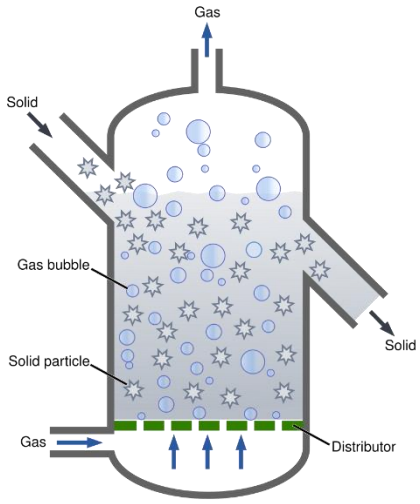

Figure 1.3.2 Basic diagram of a fluidized bed reactor. Image from Wikimedia Commons.

Currently Chemical-looping combustion has been demonstrated in various pilot plants, 1 MW_{th} [7] and 2.5 MW pseudo-CLC [8], but not yet at commercial scale. The 1 MW_{th}-experiment by Ströhle et al. at Technische Universität Darmstadt used hard coal as fuel and ilmenite as oxygen carrier. An important result from the experiments was that the oxygen demand for oxidizing unconverted gases was in line with results from smaller units. However, only partial CLC was achieved as the fuel reactor was fluidized with a mix of air and steam. Review articles that summarizes progress in the field have been written by Hossain and de Lasa [9], with the advances in CLC up to 2008 is reported; Fang et al.[10],

with advancement in development in CLC up to 2009; Adanez et al.[11], where the main advances in CLC and Chemical-Looping Reforming (CLR) up to 2010 is reported with much focus on oxygen carriers; Fan and Li [12], reported on various Chemical-Looping- Combustion, Gasification and Reforming processes 2010; Moghtaderi [13], various different Chemical-Looping processes 2012; Lyngfelt [14], reported on the status of development in CLC with solid fuels 2014; and. A books on CLC have been written by Fan [15], a more thorough of Chemical-Looping Systems compared to the review article by Fan & Li. Fennell & Anthony edited a book on Calcium and Chemical Looping Technologies with chapters by many of the leading researchers in the field[16].

Packed bed systems have also been suggested but the experimental experience is limited. [17-21]

1.3.1 Chemical-Looping Combustion with Solid Fuels

While CLC using gaseous fuel is relatively straightforward, using solid fuels comes with a few different challenges. As the fuel cannot be used as fluidization gas in the fuel reactor the reactor system has to be adapted for addition of solid fuel. When the fuel enters the fuel reactor the volatile part of the fuel can react directly with the solid oxygen carrier, but the char first needs to be gasified. For gasification and fluidization of the fuel reactor steam and/or recirculated flue gas is used converting the solid fuel to hydrogen gas and carbon monoxide, syngas. The syngas is then oxidized by the oxygen carrier. The main challenges are to gasify all char in the fuel reactor without it escaping to the air reactor or with the flue gas and to convert the syngas. These challenges need to be considered when designing a reactor system and choosing an oxygen carrier. When choosing oxygen carrier it is necessary to consider ash that is a part of solid fuels and likely will limit the oxygen carrier life time. The oxygen carrier should thus preferably be of low cost, have high reactivity with syngas and possibly have CLOU properties, which is introduced in the following section.

1.3.2 Chemical-looping with Oxygen Uncoupling (CLOU)

If the oxygen carrier is chosen so that oxygen in gas phase is released spontaneously at fuel reactor conditions (high temperature, low oxygen partial pressure), the intermediate fuel gasification step is not needed. This concept with gas phase oxygen release from the oxygen carrier is called chemical-looping with oxygen uncoupling (CLOU) and is described by reaction (5)[22].

$$Me_xO_y \rightarrow Me_xO_{y-1} + \frac{1}{2}O_2 \tag{5}$$

Oxygen released by reaction (5) will react with char in an ordinary combustion reaction without diluting the flue gas with nitrogen and the reduced oxygen carrier can be reoxidized in the air reactor via reaction (2). The sum of reactions is the same as for CLC but the slow gasification steps reaction (3) and (4) can be avoided. This makes CLOU an attractive concept for oxidation of solid fuels. However, the ability to release gaseous oxygen has been shown to be advantageous also during combustion of gaseous fuels since oxygen released may be present above the bed in the upper part of the fuel reactor and thus contribute to achieving full conversion of fuel. Mayer et al. and Abad et al. came to this conclusion after analyzing experiments made with both CLOU and non-CLOU oxygen carriers at Technische Universität Wien in a 120 kW_{th} pilot reactor [23, 24].

1.3.3 Chemical-Looping Reforming

The Chemical-Looping concept can be applied to other things than combustion for energy. The system can be adapted for syngas or hydrogen production with carbon dioxide capture. Rydén and Lyngfelt investigated different alternatives [25] and concluded that some proposed systems even might be more efficient than an reference case with conventional steam reforming.

1.3.4 Oxygen carriers

The oxygen carrier is crucial to the chemical-looping process. To select suitable oxygen carriers, several parameters should be considered. One important parameter is the reactivity toward fuels and air. A high

conversion of fuels such as natural gas or syngas is required. This requires both suitable thermodynamic properties of the oxygen carriers and sufficiently fast reaction kinetics. Physical factors which also affect the actual reaction rate include particle size, porosity, surface area etc. Another important factor is reversibility, which can be expressed for example as the number of fuel conversion cycles an oxygen carrier can undergo without deactivation. Deactivation may have several causes, e.g. that the oxygen carrier decomposes into a non-reversible state, loses porosity or reacts with sulfur from the fuel forming inert metal sulfides. Other important particle properties include resistance toward attrition and fragmentation. Moreover, factors such as melting temperature, oxygen transfer capacity, R_O, (i.e. the mass fraction of the oxygen carrier that is oxygen available for fuel oxidation), price, toxicity and environmental impact should also be considered.

The oxides of transition-metals, such as iron, nickel, copper and manganese are all potential oxygen carriers, of which copper and manganese are capable of CLOU. Combined oxides of different transition-metals are also potential oxygen carriers. For example: the iron-titanium oxide ilmenite is a material that have been extensively used as an oxygen carrier

Nickel oxide based oxygen carriers have been proven satisfactory in numerous studies: Jerndal et al. found both high fuel conversion and good fluidization behavior in freeze granulated oxygen carriers in a batch reactor [26], Linderholm et al. used spray dried particles continuously for over 1 000 h with high fuel conversion [27] , Bolhàr-Nordenkampf et al. achieved high methane conversion with spray dried particles in a 120 kW_{th} unit [28] and Adánez et al. used impregnated particles in a 500 W_{th} unit without change in particle properties [29]. However, the use of nickel oxide involves several drawbacks, such as thermodynamic constraints concerning the degree of fuel conversion, sensitivity to fuel impurities such as sulfur, and, compared to alternatives, high price and toxicity[11].

Copper oxide based oxygen carriers have demonstrated high reactivity in studies by A. Abad et al.[30], Mei et al.[31] and de Diego et al.[32]. However, drawbacks with copper oxide based materials include poor structural integrity in studies by I. Adánez-Rubio et al.[33], M. Rydén et al. [34] and loss of active material in studies by Penthor et al. [35] and de Diego et al. [32]. Also, the relatively low melting temperature of copper at 1085°C could become a problem during extended operation.

Table 1.3.4 Monometallic oxygen carriers compared by oxygen transfer capability, whether their reaction with methane is exo- or endothermic, CLOU capability, arbitrary reactivity with methane, most important shortcomings and a few references to studies. Note that nickel and copper is often together with an inert support material in an oxygen carrier making their high R_O values come closer to those for manganese and iron.

	$R_O=m_{ox}/(m_{ox}-m_{red})$	**FR reaction with CH_4**	**CLOU**	**CH_4 reactivity**	**Shortcomings**	**Ref**
CuO/Cu_2O	0.1	Exo	Yes	+++	Poor durability	[30-34]
CuO/Cu	0.201	Exo	Part	+++	Low Cu melting point Poor durability	[36]
Fe_2O_3/Fe_3O_4	0.033	Endo	No	+	Poor reaction kinetics with CH_4	[37, 38]
Mn_3O_4/MnO	0.070	Endo	No	++		[39]
Mn_2O_3/Mn_3O_4	0.034	Exo	Yes	++	Low reoxidation T Poor kinetics for oxidation	[40]
NiO/Ni	0.214	Endo	No	+++	Toxicity, CO/H2 conversion limited to approximately 99%	[26, 28, 29, 41]

A summary of monometallic oxygen carriers are shown in Table 1.3.4 where a few relevant characteristics are included. The oxygen transfer capacity, R_O, are included but note that the high values for nickel and copper get lower as they are often combined with and inert support material in an oxygen carrier. Whether the reaction with methane is exo- or endothermic is relevant for process design as an

endothermic reaction would require a higher solid circulation, in order to fulfill the thermal balance between the two reactor vessels. The reactivity is ranked compared to the other materials. The most important shortcomings are also included and they motivate looking into combined oxides as the next step in oxygen carrier evolution.

1.3.4.1 Mixed (Manganese) oxides

Focus here is on mixed oxides that includes manganese since they are shown to have CLOU capability as well as being relatively low-cost and readily available. Oxygen carriers based on manganese and iron have been studied by several researchers. Azimi et al. [42-44] found almost complete fuel conversion at very low oxygen inventory and also investigated various support materials to increase particle strength and attrition resistance, Rydén et al. [45] found high oxygen release but low attrition resistance in continuous experiments, Haider et al. [46] found significant CLOU behavior using impregnated ore particles, Shafiefarhood et al. [47] studied decomposition (i.e. reduction) temperatures on Fe-Mn oxides, Shulman et al. [48] found oxygen release characteristics as well as high reactivity with methane, Bhavsar et al. [49] investigated oxygen carriers with CeO_2 as support and Larring et al. [50] examined potential operating temperatures for different ratios of Fe-Mn. As iron and manganese are quite similar in atomic mass and ionic radius they are interchangeable in the oxides $(Fe+Mn)_2O_3$ and $(Fe+Mn)_3O_4$. Azimi et al. found in their studies that a Mn/(Mn+Fe) ratio of 0.5 – 0.8 is favourable from a thermodynamic point. At a partial pressure of oxygen of 0.05 atm the temperature change, or corresponding oxygen partial pressure change, needed for phase change at that ratio is minimal. The experiments in the studies mentioned above achieved substantial oxygen release as well as high ability to oxidize fuel. Other mixed manganese oxide have been evaluated as oxygen carriers.

Manganese have also been combined with magnesium and silicon. Examples include work by Mattisson et al. [51] who investigated different binary an ternary oxides. Källén et al. [52-54] also have investigated several materials with manganese, silicon and iron and found promising reactivity but low attrition resistance, however, a Mn-Si material with Ti addition showed no large attrition. Shulman et al. [55] investigated MnMg oxides with respect to reactivity and oxygen release and found that addition of calcium hydroxide was beneficial.

Another combined manganese oxide that has been proposed for CLC is $CaMnO_{3-\delta}$. Leion et al.[56] and Rydén et al.[57] studied $CaMn_{0.875}Ti_{0.125}O_{3-\delta}$ with results good enough to motivate further studies. Fossdal et al. investigated oxygen carriers based on low cost raw materials and found that a manganese ore with calcium addition was a promising oxygen carrier [58]. $CaMnO_{3-\delta}$ has a perovskite structure (i.e., a crystalline structure having a unit cell that can be written as $ABO_{3-\delta}$, in which A is a large cation and B is a smaller cation). The δ-factor expresses the degree of oxygen deficiency in the structure: δ=0 for a perfect structure. Materials of perovskite structure are feasible for chemical looping application because δ can be increased or reduced, while keeping the perovskite structure intact. The equilibrium δ is changed by altering factors in the surrounding such as temperature, pressure, or oxygen fugacity (see the work of Leonidova et al. [59]). The surroundings in a chemical-looping air reactor are oxidative, while they are reductive in the fuel reactor. Therefore, the value of δ_{AR} will be smaller and that of δ_{FR} will be larger. The amount of oxygen available for oxidation of fuel can be written as $\delta_{FR} - \delta_{AR}$. The A and B sites do not have to consist of one single type of ion. Doping of the A-site and the B-site with one or more types of ions is possible as long as the dopants have similar ionic radii and oxidation state as the main atom. The B site can be selected among most transition metals. Good candidates for the application of CLC could be, for example, manganese, iron, and titanium. The A-site must have much larger ionic radii, so there are less options. Calcium appears to be the most attractive for the A-site because of good availability and low cost. The general criteria concerning the formability of perovskites has been extensively reviewed by Li et al.[60]. Another notable feature of $CaMnO_{3-\delta}$ is the fact that the sum of reactions in the chemical-looping fuel reactor will be slightly exothermic, which could be advantageous, with respect to heat balance of a chemical-looping facility. Reaction enthalpy for oxygen release from $CaMnO_{3-\delta}$ materials have been examined by Rørmark et al.[61] and kinetics by Abad et al. [62]. Not all materials with a perovskite structure undergo changes under conditions relevant for

chemical-looping combustion, but $CaMnO_{3-\delta}$ based materials have been shown to do so, as well as materials substituted with lanthanum and iron[63]. The study of Bakken et al. of $CaMnO_{3-\delta}$ showed that there may be reversible decomposition to $Ca_2MnO_{4-\delta}$ and $CaMn_2O_{4-\delta}$[64]. In the materials tested in paper II, some of the manganese was substituted by titanium, iron, or magnesium. Galinsky et al.[65] investigated manganese substitution with aluminum, vanadium, iron, cobalt and nickel, iron was deemed most suitable as it was fully compatible with the perovskite structure while the other dopants formed secondary phases. Also calcium substitution have been investigated by Galinsky et al.[66], of barium and strontium the strontium was found to effectively stabilize the perovskite structure. Arjmand et al. [67] have studied $CaMnO_{3-\delta}$ based oxygen carriers with lanthanum as A-site dopant and iron, titanium, magnesium or copper as B-site dopant. All variants performed well except for the material doped with copper that defluidized. Arjmand et al. [68] and Cabello et al. [69] have investigated the sulfur tolerance of these oxygen carriers. Arjmand et al. found that while presence of sulfur dioxide reduced reactivity it could be minimized by adjusting operating parameters while Cabello et al. found that hydrogen sulfide addition to fuel substantially reduced reactivity as well as caused agglomeration problems. Schmitz et al. [70] have done continuous experiments with $CaMn_{0.9}Mg_{0.1}O_{3-\delta}$ using sulfurous solid fuels, and while the performance was superior compared to ilmenite, a reversible loss of reactivity was noticed. Schmitz et al. [71] also investigated the same material in a longer experiment using biochar with very good results. $CaMnO_{3-\delta}$ based oxygen carriers have also been used for Chemical-looping combustion with liquid fuel by Moldenhauer et al. [72, 73], in these experiments the fuel conversion was high but not complete.

1.4 Aim of work

As the work in Paper I is not on $CaMnO_{3-\delta}$ as Papers II-IV, the aim of Paper I is here presented separately.

1.4.1 Paper I

In chemical-looping combustion of solid fuels a lower oxygen carrier life time is expected due to possible deactivation by ash and loss of oxygen carrier in the removal of ash. The lower cost of a naturally occurring mineral, compared to a designed and manufactured oxygen carrier, should be more suitable for solid fuel. Ilmenite is a naturally occurring mineral, which has been used as oxygen carrier material for solid fuels. The overall redox reaction of ilmenite in chemical-looping combustion would be reaction (6).

$$4FeTiO_3 + O_2 \leftrightarrow 2Fe_2TiO_5 + 2TiO_2 \quad (6)$$

Ilmenite is a combined oxide for which reliable thermodynamic data is not readily available. Due to uncertainty regarding intermediates in that reaction and a reported segregation of iron and titanium oxide in the oxygen carrier particles [74] the reaction enthalpy needed to be verified.

1.4.2 Paper II-V

Because of earlier mentioned drawbacks with nickel, the development of oxygen carrier materials without nickel is well motivated. Paper II, III IV and V was part of a larger project, Innocuous, with the goal to development an oxygen carrier without or with little nickel for combustion of natural gas. The general material development strategy used in the project is shown in Figure 1.4.2. A large number of materials were prepared in step 1 and 2. All of those materials underwent step 3c and those with sufficient crushing strength also step 3a and 3b. The jet cup test in step 3d was developed in parallel but was included in the developing scheme in the Success project, which eventually followed the Innocuous project. Paper II-V describes part of the development effort in the aforementioned project. Paper II includes a part of step 3 but discussion about all of the 79 materials that was manufactured is included in a paper by Jing et al. [75]. Of the mentioned 79 materials 10 were deemed promising and continued to step 4 and 5. Part of step 5 is included in Paper III and V and additional work on that were made by Rydén et al.[34] and Källén et al.[54]. Of the 10 materials from step 5 only 2 proceeded to step 6 and 7.

Step 7 is included in Paper IV and in work by Källén et al.[76]. Additional work from Innocuous can be found in studies by Sundqvist et al. [77], Jing et al. [78, 79],Rydén et al. [80], Mattisson et al. [81].

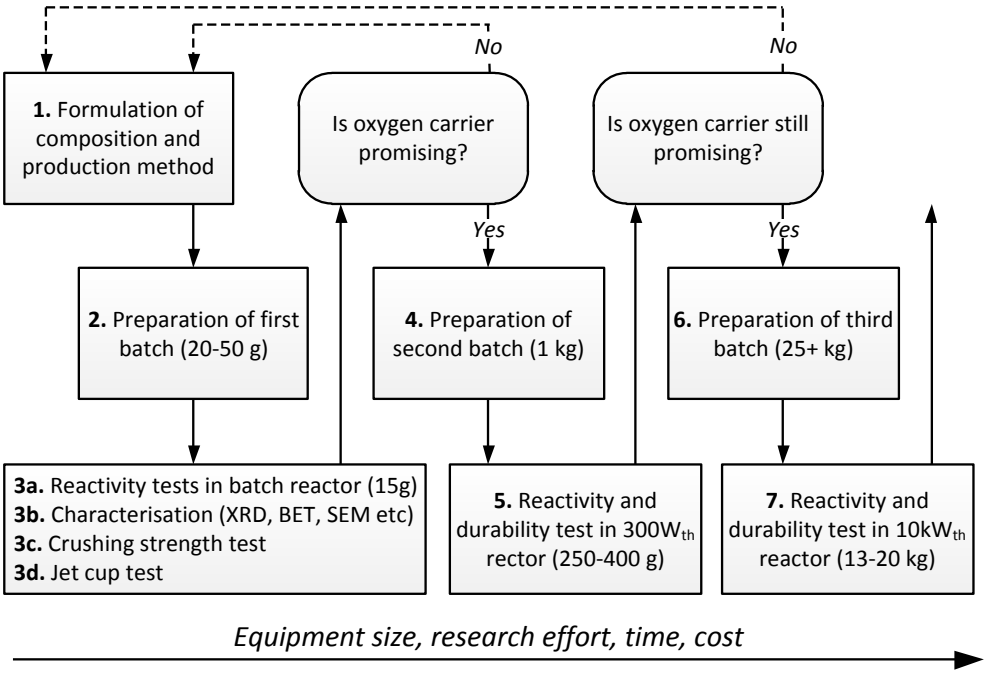

Figure 1.4.2 Oxygen carrier developing scheme. From Rydén et al. [82]

The ultimate goal of the Innocuous project and the Success project was the development of industrially feasible oxygen carrier materials with low cost and low environmental impact, as well as manufacturing methods for particles suitable for use in fluidized bed reactors. Paper II-V constitutes a significant contribution towards this goal.

2. METHOD AND MATERIAL

To be able to determine the viability of an oxygen carrier material many characteristics needed evaluation.

- Poured bulk density was determined with a standardized pouring devise and a scale. The value was used to decide the amount of particles to use in the continuous units.
- Particle size distribution was obtained by placing a representative weighed sample on a column of sieves with mesh cloth with openings in different, defined sizes. The column of sieves was placed in a mechanical shaker and after a set time the content of each sieve was weighed. How the particle size distribution developed during continuous operation was used as a measure of particle structural integrity.
- The force required to crush a particle was determined using a digital force gauge. The values for individual particles differed substantially and therefore an average of 30 particles were used. This crushing strength was used as a measure of the mechanical strength of the particles.
- An ocular assessment of particles where shape and possible micro agglomerations could be discovered was made using a light microscope.
- X-ray crystallography was used to investigate the crystal composition of materials.

2.1 Experimental setup

Three different setups have been used for the experiments covered in this thesis. A comparison between the reactor systems is shown in table 2.1. They are all fluidized bed systems. Also common for all of the systems is that they utilize electrical heating in order to perform the experiments at desired temperature. Outlet gases are analyzed with a multicomponent gas analyzer after being subject to condensate removal and filtering.

Table 2.1 A comparison between the reactor systems. The operating time refer to a typical experiment with one material. The amount of bed material for the continuous units is dependent on the bulk density of the material and does not include the material possibly needed to make up for samples and fragmentation. The number of materials tested are total for the unit, not by the author. The gas velocity is when comparing the units to each other.

Reactor system	Operating time	Mass of bed mtrl [g]	Process	# mtrl tested	Gas velocity
Batch	Hours	15	Batch	Hundreds	Low
300 W	Days	250 - 400	Continuous	Dozens	Intermediate
10 kW	Weeks	9 000 – 17 000	Continuous	Few	High

2.1.1 Fluidized bed batch reactor

A fluidized-bed reactor of quartz is placed inside an electric oven. The oven is insulated and the opening through which the gases entered and exited the reactor are insulated with quartz wool. The quartz reactor is cylindrical and has an inner diameter of 22 mm and a height of 870 mm. The oxygen carrier is placed on a porous quartz plate located 370 mm from the lower end. Fifteen gram of oxygen carrier or sand is the amount used for all experiments. Temperature measurements are conducted with two CrAl/NiAl thermocouples enclosed in Inconel 600 in quartz shells. The thermocouples are located 28 mm below the porous plate in order to measure temperature below the bed, and 22 mm above for measurements in the bed. The experiments were performed at 900 – 1000 °C, as measured by the upper thermocouple. The pressure drop over the reactor is measured with a frequency of 20 Hz in order to determine whether the bed is fluidized or not. The experiments were run in cycles where the fluidizing gas was alternated between oxidizing and reducing with a purging inert in between. A schematic picture of the setup is shown in Figure 2.1.1.

The most important advantages with the unit include: a very small amount of oxygen carrier needed, experiment takes only hours, hundreds of oxygen materials have been tested in this setup and are available for comparisons, easy to control oxidation and reduction, few things to cause problems. A disadvantage is that running multiple cycles is quite time consuming.

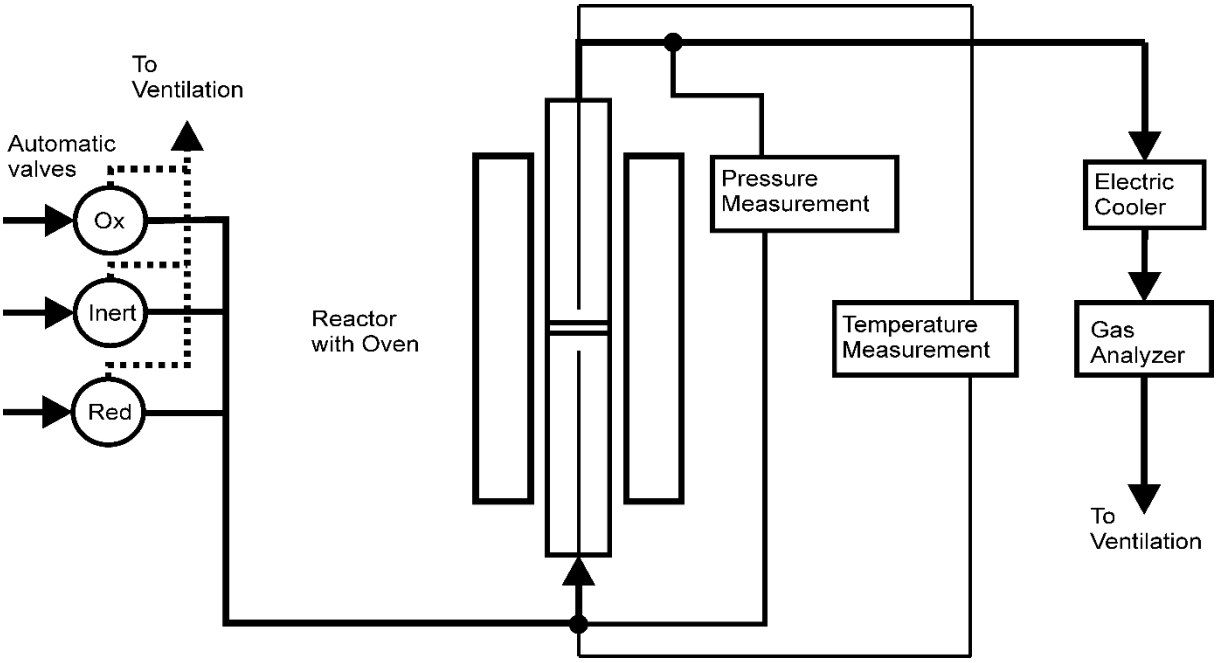

Figure 2.1.1 Schematic picture of the fluidized batch reactor setup

2.1.2 300 W Chemical-Looping Combustor

The reactor is designed to use a rather small amount of oxygen carrier with gaseous fuel. Worth noting is that 300 W is the original fuel power for which the reactor was designed using natural gas as fuel, but during experiments fuel power is typically varied on purpose. The amount of oxygen carrier required to operate the reactor depends on the density of the oxygen carrier and is in the range 200 – 400 g. The inner dimensions of the air reactor are 25 * 42 mm in the base and decrease to 25 * 25 mm in the riser section. The inner dimension of the fuel reactor is 25 * 25 mm. The inner dimensions of the downcomer are 21 * 44 mm. Two 3D images of the reactor from different directions are shown in Figure 2.1.2. The gas to the air reactor and fuel reactor enters wind boxes and is evenly distributed over the cross section by porous quartz plates. In the downcomer and bottom loop seal (slot) gas enters through the pipes seen in Figure. These inlets are divided in two so that one inlet is on the fuel reactor side and the other is on the air reactor side. The gas is distributed through small holes drilled in the pipes directed downwards. The air flow in the air reactor is sufficiently high to throw the particles upwards to a wider settling zone (not shown in figure) where they fall down. A fraction of the falling particles enters the downcomer loop seal. Via the return orifice they fall into the bubbling fuel reactor where they are reduced. From the bottom of the fuel reactor the particles enter the slot loop seal and return to the air reactor where they are reoxidized and the loop is completed. The oxygen depleted air from the air reactor passes through particle filter while the flue gases from the fuel reactor pass through a particle filter and water seal, before leaving the reactor system. Slip streams are extracted after both the air reactor and the fuel reactor and are taken to gas conditioning systems, in which each slip stream is further filtrated and water is condensed. Following the gas condition systems the concentrations of O_2, CO_2, CO and CH_4 are measured continuously using a combination of infrared and paramagnetic sensors. N_2 and H_2 from the fuel reactor are measured periodically by gas chromatography. The gases in the air reactor and fuel reactor are somewhat diluted by the gas that fluidizes the slot. The gases are furthermore diluted with the gas from the downcomer when it leaves the reactors and dry gas concentrations measured are thus slightly lower than when leaving the reactor. Both the downcomer and slot were fluidized with argon.

The advantages with this reactor are the continuous operation, the fairly small amount of oxygen carrier needed and that experiments only take days to carry out. Disadvantage with this system is that it is difficult to determine the oxygen carrier flow between air and fuel reactor and thus knowing the degree of reduction/oxidation of oxygen carriers.

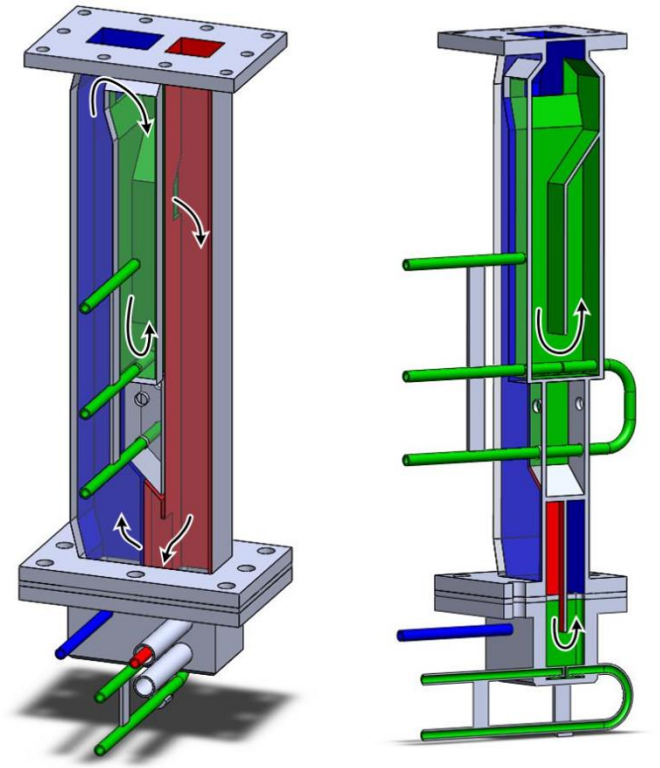

Figure 2.1.2 The 300 W Chemical-Looping Reactor. Arrows show the direction of oxygen carrier flow. The blue part is the air reactor, the red part is the fuel reactor and the green parts are the downcomer and slot. Image courtesy of Patrick Moldenhauer.

2.1.3 10 kW Chemical-Looping Combustor

The reactor has a nominal thermal power of 10 kW_{th} with natural gas. A schematic image of the setup is shown in figure 2.1.3.1. An air reactor that eventually narrows in-to a riser drives the circulation of solids. After the riser, gas is separated from particles in a cyclone. From the cyclone the particles fall down into a particle loop seal that prevents gas leakage between the air- and fuel-side. Below the loop seal particles continue down into a bubbling fuel reactor. On the other side of the fuel reactor an overflow exit leads the particles, via the next loop seal, back to the air reactor. A vertical plate in the middle of the fuel reactor prevents particles from by-passing the bed. The gas that leaves the cyclone and fuel reactor is first passively cooled in finned pipes before sample streams are withdrawn and led to a gas conditioning system. The gas from the cyclone is led to a bag filter that captures the elutriated particles before the gas exits to the chimney. The gas form the fuel reactor goes through a water seal with the dual purpose of collecting condensed steam and elutriated particles while also controlling the pressure

in the fuel reactor. Figure 2.1.3.2 shows a photography of the reactor system prior to insulation which clearly shows the heating coils and the many pressure taps.

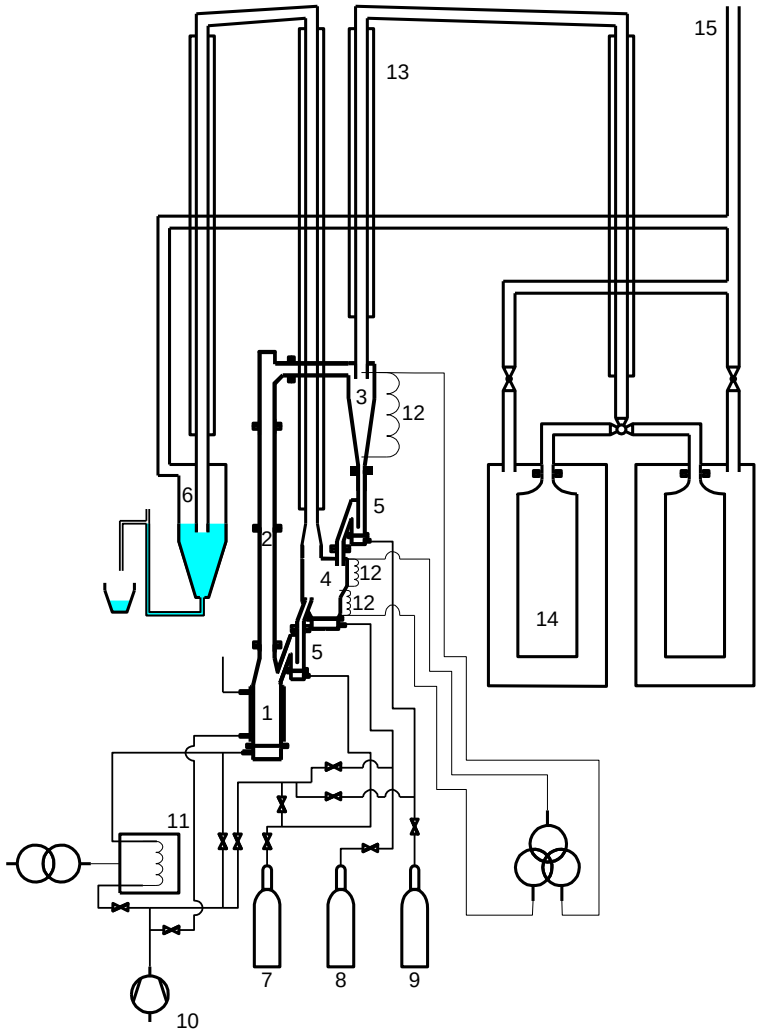

Figure 2.1.3.1 10 kW Chemical-Looping Combustor Experimental Setup with numbers as follows: 1. Air reactor 2. Riser 3. Cyclone separator 4. Fuel reactor 5. Loop seals 6. Water seal 7. Nitrogen 8. Natural gas 9. Nitrogen 10. Compressed air 11. Air preheater 12. Heating coils 13. Cooling flanges 14. Bag filters 15. Chimney. The image comes from Linderholm et al., 2008 [41].

The advantages with this reactor setup is the continuous operation, the high gas velocities (almost comparable to a commercial size unit) and that it can be operated unmanned (in a best case scenario). The disadvantages include that it is quite time consuming to set up the system, and the experiments takes

weeks (or even months) to execute. Also many different factors can cause problems in the system and a large amount of oxygen carrier (10-20 kg) is needed.

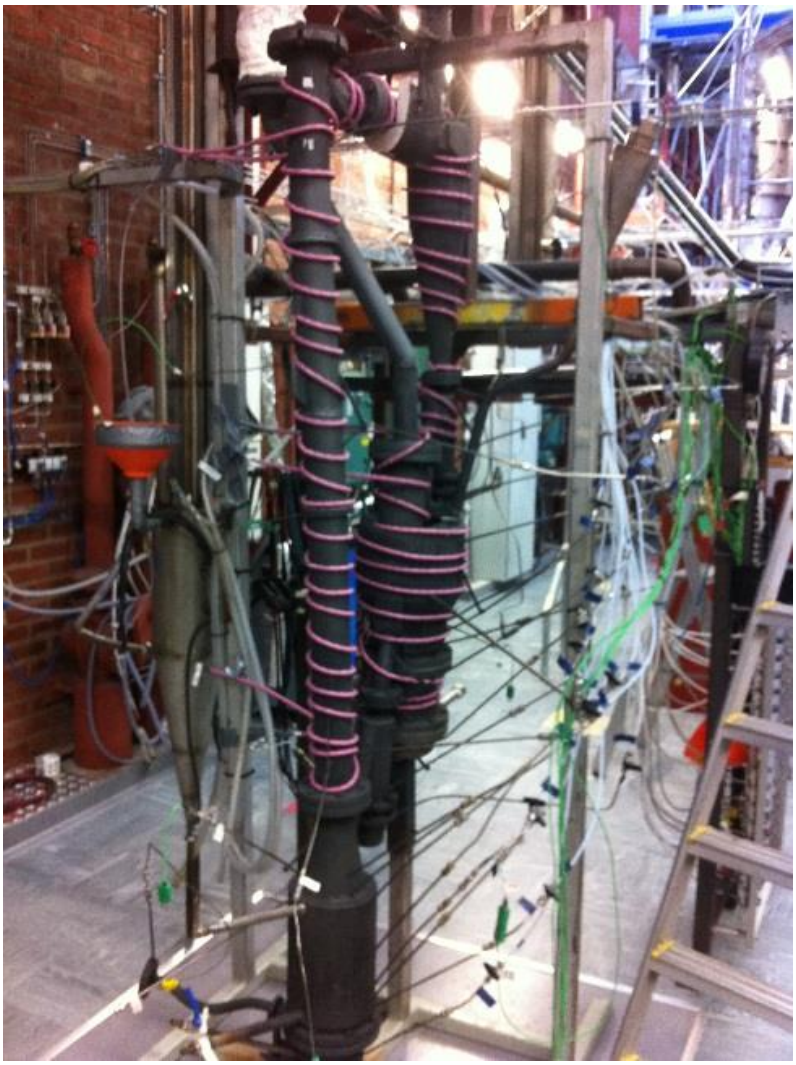

Figure 2.1.3.2 A photography of the reactor system with the pink heating coils prior to insulation.

2.2 Method

Due to the fact that the studies in the different papers were carried out on different reactor systems the method differed quite a lot. This section will briefly describe the method from each paper.

2.2.1 Determination of reaction enthalpy (Paper I)

The two main reactions in the fuel reactor is the reduction of the oxygen carrier and oxidation of fuel. Depending on both which fuel and which oxygen carrier that is being used the net enthalpy can be exothermic or endothermic. By using mixtures of fuels with known, and different, oxidation enthalpy the enthalpy of oxygen carrier reduction could be found. Seven mixtures of methane and carbon monoxide were used. By examining the reactants and the response in reactor temperature change the enthalpy of oxygen carrier reduction was established iteratively.

2.2.2 Material screening (Paper II)

The materials were tested in the fluidized batch reactor. As both the capability to release gas phase oxygen as well as reactivity with methane was of interest both of these characteristics were examined. First four cycles with nitrogen as reducing gas, then three cycles with syngas, three cycles with natural gas and finally three more cycles with nitrogen. The final cycles with nitrogen were to determine if the reactions with fuel had affected the ability to release oxygen. An overview of the experimental plan is

presented in table 2.2.2. Beyond the chemical properties the fluidization behavior and the mechanical durability of the particles were of interest.

Table 2.2.2 Experimental plan for oxygen uncoupling and fuel reactivity testing. F_i is flow in the period i, i.e. Oxidation, Reduction and Inert. t_i is the time for period i. T is temperature.

No of cycles	Reducing gas	F_{Ox} [mL_N/min]	F_{In} [mL_N/min]	t_{In} [s]	F_{Red} [mL_N/min]	t_{Red} [s]	T_{Ox} [°C]	T_{Red} [°C]
3	nitrogen	900	600	360	-	-	900	900
1	nitrogen	900	600	360	-	-	900	900 → 1000
3	methane	900	600	60	450/360	20	950	950
3	syngas	900	600	60	450/360	80	950	950
3	nitrogen	900	600	360	-	-	900	900
2	nitrogen	900	600	360	-	-	900	900 → 1000
1	nitrogen	900	600	1800	-	-	900	900 → 1000

2.2.3 300 W Chemical-looping Combustor (Paper III and V)

The experiments in this unit were carried out over several days. During the first days the CLOU capability was examined as temperature was stepwise increased. While CLOU was examined the fluidization gas in the slot loop seal and downcomer was argon and in the fuel reactor carbon dioxide. The air reactor was fluidized with air, or air diluted with nitrogen to an oxygen concentration of 5 %. The choices of fluidization gases was in order to be able to notice any leakage between the air reactor and fuel reactor. The difference in oxygen concentration in the oxidation gas was to determine whether that would influence the degree of oxidation (i.e. the δ-factor) of the oxygen carriers as expected. After the CLOU testing the following days were spent on operation with natural gas. Initially natural gas diluted with nitrogen was used not make sure nothing weird happened. After that several different values of the parameters air reactor flow, fuel flow and fuel reactor temperature were examined.

2.2.4 10 kW Chemical-looping Combustor (Paper IV)

The goal with this campaign was long term testing and verification of the oxygen carrier under conditions roughly comparable to future industrial units. Different values of the parameters fuel reactor temperature, solids inventory, air and fuel reactor flow was tested in order to find stable settings for continuous operation. An overview of the campaign is presented in Table 2.2.4.

Table 2.2.4 Overview of the experimental campaign. The temperature displayed was measured by a thermocouple in the bottom of the fuel reactor and the values below 900 °C occurred during heat-up periods with fuel addition at the beginning of some days.

Day	Time with fuel [h]	Nominal solids inventory [kg]	Air flow [L_N/min]	Fuel flow [L_N/min]	Temperature [°C]
1	0.4	13	200	9	870
2	15.4	13	180	8-9	940-950
3	12.6	13	160	8-10	940-950
4	11.9	13	160-200	7-10	930-950
5	5.2	13	160-200	6-8	700-950
6	3.1	13	160-170	4-7	940
7	8.0	13	180-200	8	900-930
8	9.5	14	160-180	7-8	920-950
9	11.2	14	160	7	910-930
10	6.1	14	160	7	800-920
11	3.8	14	160	7	800-930
12	12.2	14	160	7	930-950
Sum:	99				

2.3 Data evaluation

A few different characteristics were evaluated from the experiments. The conversion of fuel was measured as

$$\gamma = \frac{x_{CO_2}}{x_{CO_2} + x_{CO} + x_{CH_4}} \tag{6}$$

Where x_i being the fraction of specie i. That was a very simple measure of how much of the fuel was oxidized to carbon dioxide and as such it is called CO_2 yield. It was measured from gases leaving the fuel reactor and does not take into account possible gas leak to air reactor or coking. During batch tests the reduction of the oxygen carrier was an important measure,

$$\omega = \frac{m}{m_{OX}} \tag{7}$$

Was generally used where m is current mass of oxygen carrier and m_{OX} is the mass of the fully oxidized oxygen carrier. During the continuous experiments attempts were made to quantify the attrition of the particles by measuring the particles below 45 µm that was produced. Generally particles added were in the size range 106-212 µm. The attrition of the material during operation was expressed as

$$A = \frac{m_{<45\mu m}}{m_{tot} * t} \tag{8}$$

Where $m_{<45\mu m}$ was the mass of fines, m_{tot} the total solids inventory and t the total operation time with fuel fluidizing the fuel reactor. The inverse of the attrition is a value for expected particle life time.

2.4 Oxygen carriers

In paper I the experiments were focused on ilmenite based oxygen carrier. Ilmenite is an iron-titanium oxide that requires limited processing to be used as oxygen carrier. Being an ore it was low-cost but unfortunately the reactivity with methane is rather low so it is unsuitable as an oxygen carrier for natural gas. All other papers focused on chemical-looping combustion with natural gas hence other oxygen carriers was looked into. Paper II was a part of a larger screening where 79 different oxygen carriers were manufactured and evaluated. The method of production was spray drying as it, as a well know production method for powders and small particles, were deemed possible to scale up in later stages of the project. The particles could be divided in three larger groups of particles with either Cu, CaMn or MnMg as active material. A few of the materials based on Cu and CaMn performed quite well with regard to CLOU capability and fuel reactivity in batch reactor. However many materials had low mechanical strength and were disqualified from batch reactor evaluation. Of the materials with best mechanical and reactivity properties 10 were produced in larger batches for continuous operation in larger pilot reactor. The Cu-based oxygen carrier suffered high attrition and deteriorating mechanical strength during continuous testing while the CaMn-based oxygen carriers proved to be more durable. Two of the CaMn-based oxygen carriers were thus chosen to be scaled up further for testing with commercially relevant gas velocities over longer time as the next step.

3. RESULTS

3.1 Determination of reaction enthalpy, Paper I

It was shown that it was possible to determine the reaction enthalpy of an oxygen carrier oxidation/reduction using a fluidized batch reactor, a thermocouple, a gas analyzer and various mixtures of reacting gases. The known reaction enthalpy of a Ni-based oxygen carrier was determined within error range with the method developed. The change in enthalpy for the sum of all the reactions that happened during the fuel cycle as a function of the change in temperature for the Ni-based oxygen carrier is shown in Figure 3.1.1. Each pair of dots in the figure are the values for one specific mixture of carbon monoxide and methane. The method was subsequently used to find the reaction enthalpy of three different ilmenite-based oxygen carriers. The results were 453 kJ (mol O_2)$^{-1}$ for a synthetic ilmenite, 469 kJ (mol O_2)$^{-1}$ for a natural ilmenite and 468 kJ (mol O_2)$^{-1}$ for another natural ilmenite that had previously been in operation in an experimental reactor. The results fit well with the suggested reaction path.

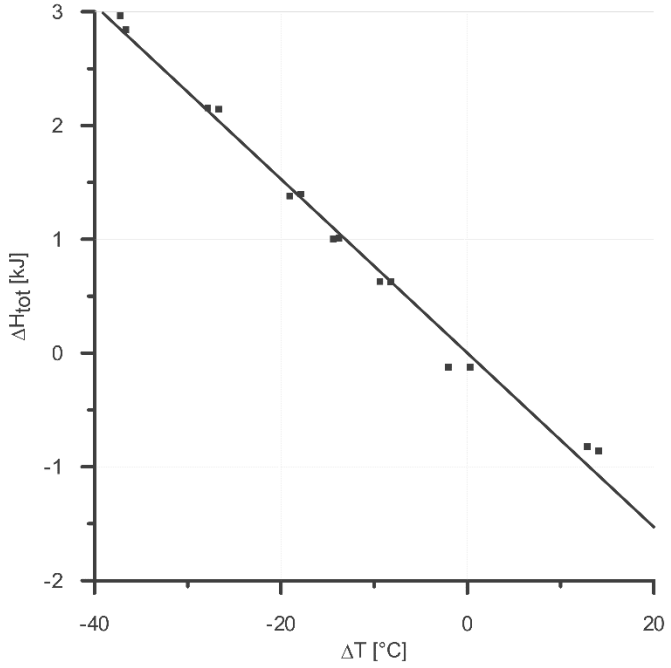

Figure 3.1.1 ΔH vs. ΔT for the Ni-based oxygen carrier and a linearization of the fit

3.2 Screening, Paper II

In paper two a part of the larger screening in the EU project Innocuous is presented. 6 different compositions of a $CaMnO_3$-based oxygen carrier doped with either iron, titanium or magnesium are compared. Each composition is produced with three different calcination temperatures; 1100, 1200 and 1300 °C. First the mechanical strength was tested by measuring the crushing strength. A higher calcination temperature resulted in a higher density and crushing strength. The materials were thereafter examined in the fluidized batch reactor with respect to oxygen release and fuel reactivity. During the batch experiments the materials with lowest crushing strength and density all formed some dust, which was found in the quartz wool used as filter, which indicated a poor durability. The threshold for dust formation was between 1.11 and 1.28 N. The four materials with highest density all showed defluidization at certain conditions during the batch experiments. The defluidization was reversible but it was found that the oxygen carriers had agglomerated. The agglomerations ranged from small micro agglomerates of a few particles to most of the bed being agglomerated. The particles that were doped with magnesium and calcined at 1300 °C had no problems during operation. All of the materials tested released oxygen to inert atmosphere and were able to fully oxidize syngas. The reactivity with methane

was higher for materials calcined at lower temperature. The reactivity of the materials calcined at 1300 °C was nevertheless quite high, some examples are shown in Figure 3.2.1. During these experiments no deterioration of the reactivity was observed which is displayed in Figure 3.2.2 were the release of oxygen from the first and last cycles were seemingly identical. A summary of the results is shown in Table 3.2.1.

Table 3.2.1 Summary of results. The materials are presented with a short name as well as composition. The crushing strength values are shown for each calcination temperature, remaining data only for materials tested in batch reactor. The average fuel conversion, γ, for a particle degree of oxidation, ω, between 1 and 0.99. Also shown are whether the particles defluidized and formed dust during batch testing. Materials C9, C12 and C14 calcined at 1100 °C were not tested in the batch reactor as they were expected to form dust as well and thus not be suitable for further studies.

calcination temperature [°C]	crushing strength [N]	γ for ω: 1 - 0.99 [-]	defluidization [yes/no]	dust formation [yes/no]
		C9		
		$CaMn_{0.75}Ti_{0.25}O_{3-\delta}$		
1100	0.46			
1200	0.63	0.97	no	yes
1300	1.3	0.91	yes	no
		C10		
		$CaMn_{0.95}Ti_{0.05}O_{3-\delta}$		
1100	0.46	0.99	no	yes
1200	0.68	0.98	no	yes
1300	1.29	0.96	yes	no
		C11		
		$CaMn_{0.8}Fe_{0.2}O_{3-\delta}$		
1100	0.39	0.99	no	yes
1200	1.11	0.95	no	yes
1300	1.43	0.90	yes	no
		C12		
		$CaMn_{0.9}Fe_{0.1}O_{3-\delta}$		
1100	0.4			
1200	0.97	0.95	no	yes
1300	1.38	0.95	yes	no
		C13		
		$CaMn_{0.8}Mg_{0.2}O_{3-\delta}$		
1100	0.36	1.00	no	yes
1200	0.65	0.97	no	yes
1300	1.28	0.99	no	no
		C14		
		$CaMn_{0.9}Mg_{0.1}O_{3-\delta}$		
1100	0.27			
1200	0.56	0.99	no	yes
1300	1.38	0.99	no	No

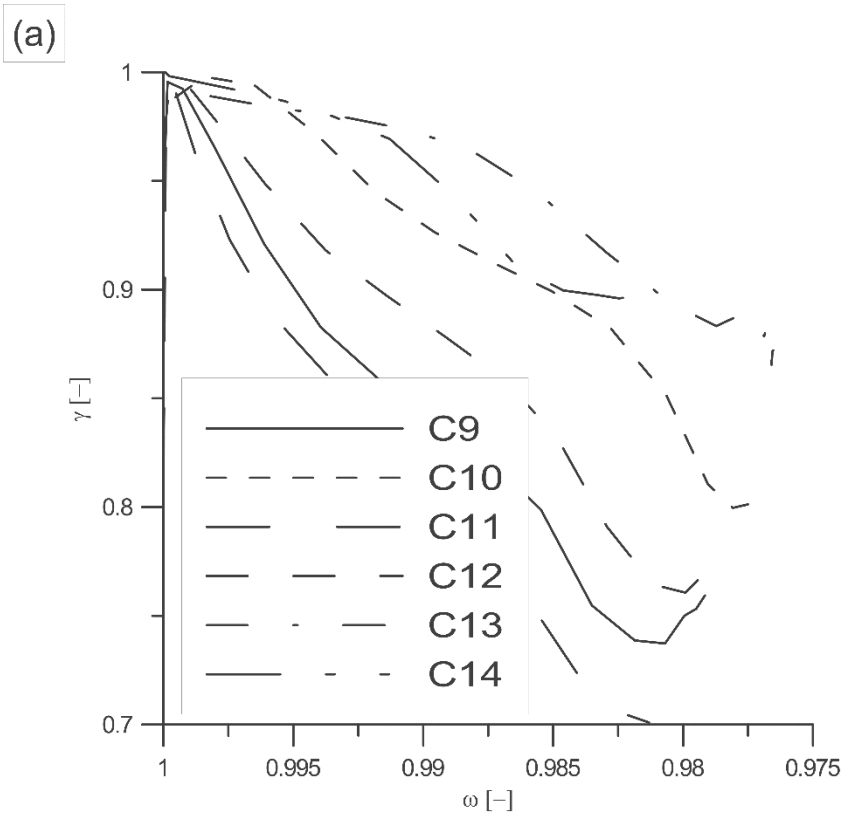

Figure 3.2.1 Reactivity with methane shown as γ against ω for particles calcined at 1300 °C.

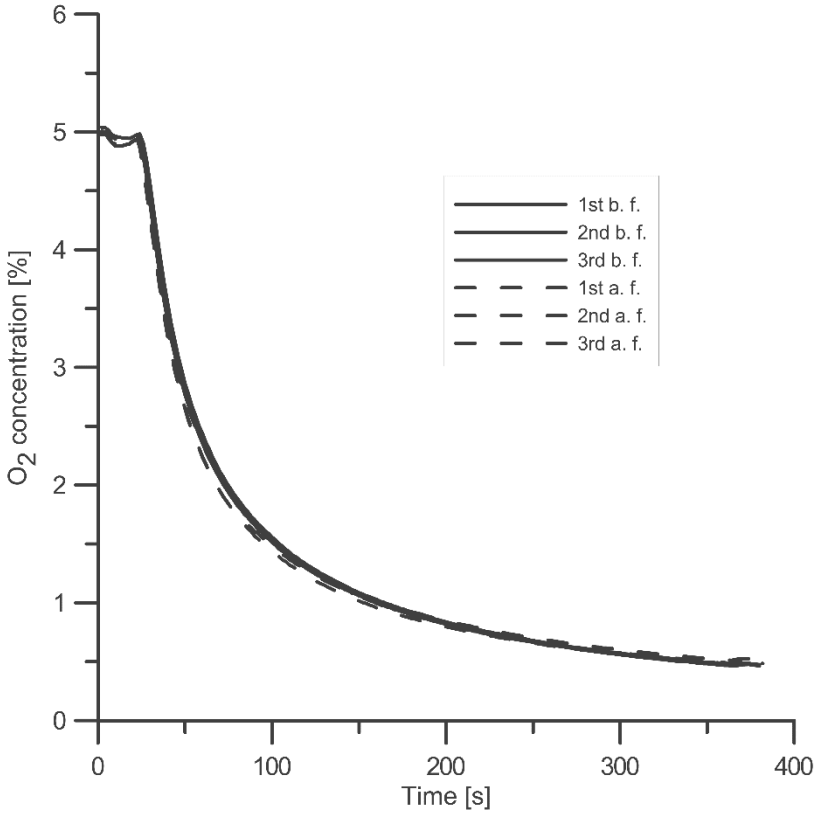

Figure 3.2.2 A comparison of the oxygen release prior, cycles 1, 2 and 3 b. f. , and post fuel , 1, 2 and 3 a. f. , cycles for $CaMn_{0.95}Ti_{0.05}O_{3-\delta}$. The graphs for all other materials looked similar.

3.3 300 W (Paper III and V)

Three different materials were examined in paper III and two in paper V in the circulating dual fluidized batch reactor. The oxygen uncoupling capacity was examined by using an inert gas instead of fuel in the fuel reactor for two different oxygen concentrations, 21 % and 5 %, for the fluidization of the air reactor. The release of oxygen to inert atmosphere in the fuel reactor was substantial. The amount of oxygen released was dependent both on temperature and the oxygen partial pressure in the air reactor as can be seen in the graphs in Figure 3.3.1. High temperature and high oxygen partial pressure in the air reactor clearly was beneficial, as could be expected.

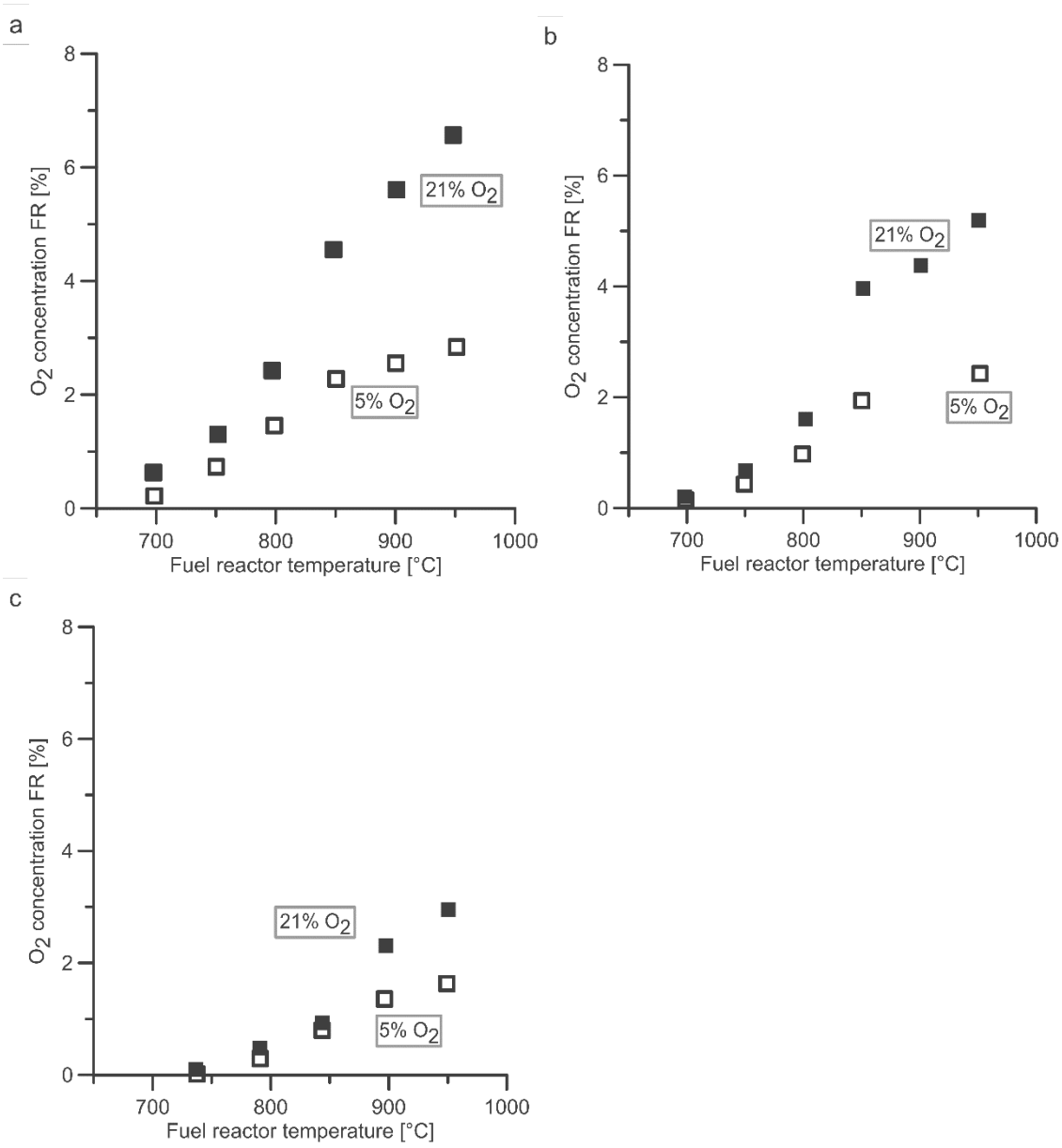

Figure 3.3.1 Effect of temperature and air reactor O_2 concentration on oxygen uncoupling for $CaMn_{0.8}Mg_{0.2}O_{3-\delta}$ (a), $CaMn_{0.9}Mg_{0.1}O_{3-\delta}$ (b) and $CaMn_{0.775}Mg_{0.1}Ti_{0.125}O_{3-\delta}$ (c).

Reactivity with natural gas was tested at 900 or 950 °C and for four of the materials the temperature dependence was tested in a temperature stair from 700 to 950 °C. The temperature was found to be a

very important parameter. The temperature dependence of fuel conversion is shown in Figure 3.3.2, note that fuel conversion is essentially complete at 900 and 950 °C.

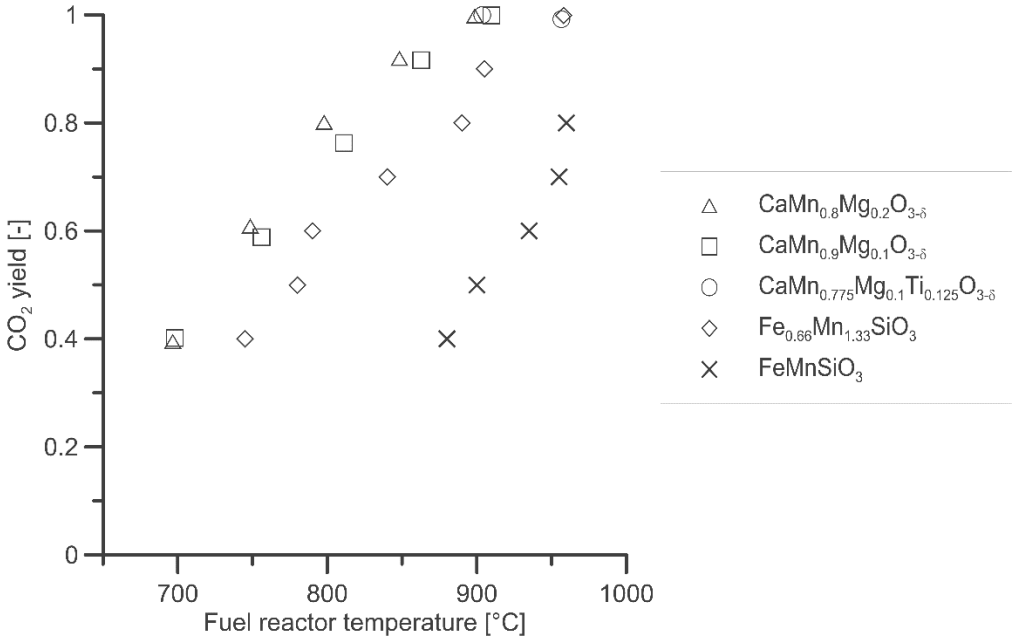

Figure 3.3.2 Effect of temperature on combustion efficiency for the used materials. The plotted values are averages for 15 min operation at each temperature.

The load of particles as function of thermal power was another important parameter and was varied by changing fuel flow. In Figure 3.3.3Figure 3. the fuel conversions are shown as a function of the solids inventory of the fuel reactor per fuel power; kg/MW_{th}. The particle load per fuel power was adjusted by changing the fuel flow. A higher particle load per fuel power, i.e. lower fuel flow, resulted in higher CO_2 yield. Worth noting is that $CaMn_{0.8}Mg_{0.2}O_{3-\delta}$ had lower solids inventory than $CaMn_{0.9}Mg_{0.1}O_{3-\delta}$ which had lower solids inventory than $CaMn_{0.775}Mg_{0.1}Ti_{0.125}O_{3-\delta}$. The differing solids inventory was because solids inventory was decided from the density of the particles. $Fe_{0.66}Mn_{1.33}SiO_3$ had a very low particle load per fuel power but at a higher temperature.

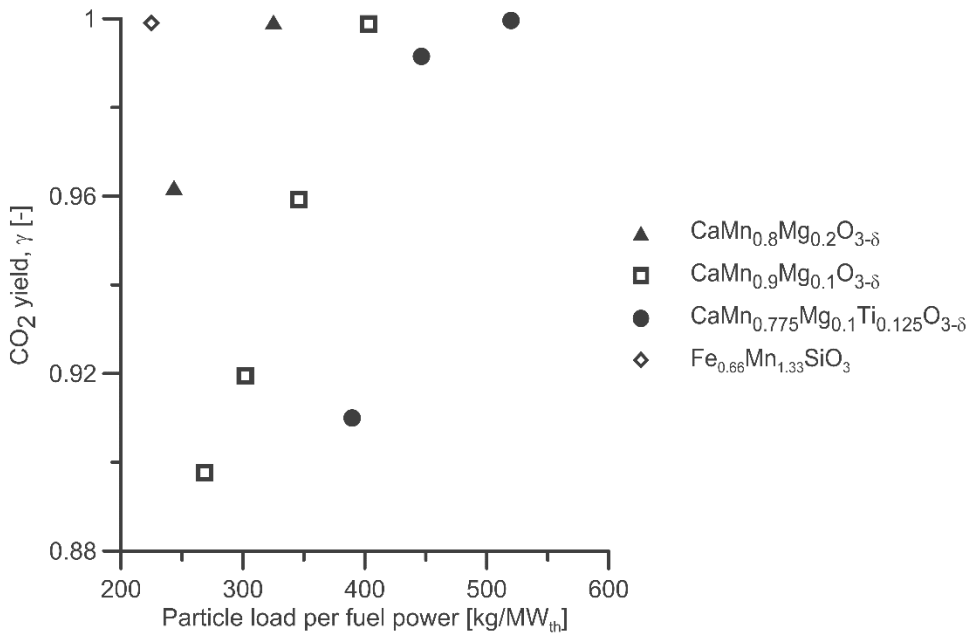

Figure 3.3.3 CO_2 yield as a function of solids inventory in fuel reactor per fuel power. The load was changed with the volumetric fuel flow and it was assumed that 26 % of the total inventory was located in the fuel reactor. Each data point is an average of 15 min operation at steady-state at 900 °C in the fuel reactor except for $Fe_{0.66}Mn_{1.33}SiO_3$ were the temperature was 950 °C. $FeMnSiO_3$ is not included as the CO_2 yield was much lower.

How the continuous operation affected the particles was considered of being of high importance. The durability was quantified by measuring how much fines, i.e. particles smaller than 45 µm, was formed during the experiments as function of time. This value was expressed as wt% loss/h of operation with fuel. For $CaMn_{0.8}Mg_{0.2}O_{3-\delta}$ the loss of fines was 0.13 %/h while for $CaMn_{0.9}Mg_{0.1}O_{3-\delta}$ it was as low as 0.03 %/h. $CaMn_{0.775}Mg_{0.1}Ti_{0.125}O_{3-\delta}$ that had an operating time of 40 h compared to 17 h for $CaMn_{0.9}Mg_{0.1}O_{3-\delta}$, had a loss of 0.08 %/h. The durability for the FeMnSi based oxygen carriers was worse. The loss of fines for $Fe_{0.66}Mn_{1.33}SiO_3$ was 4.2 %/h and for $FeMnSiO_3$ 1.2 %/h.

$CaMn_{0.775}Mg_{0.1}Ti_{0.125}O_{3-\delta}$ was also examined in change of size distribution and the changes were quite small as shown in Figure 3.3.4. This small change can be due to a swelling of particles of even just an artefact.

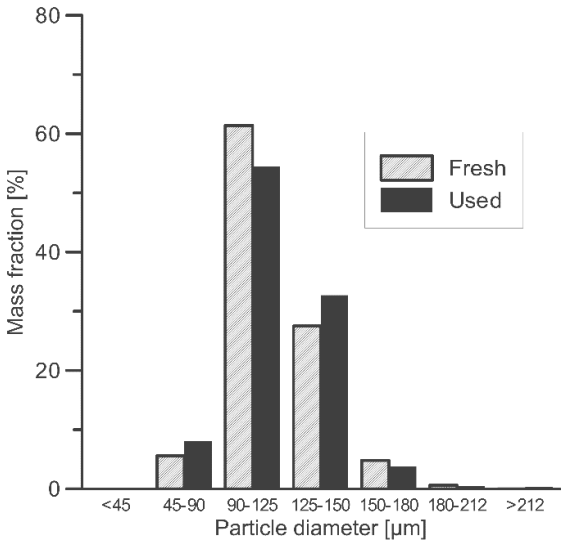

Figure 3.3.4 Particle size distribution for $CaMn_{0.775}Mg_{0.1}Ti_{0.125}O_{3-\delta}$, comparison between fresh particles added to reactor and the retrieved used ones.

The chemical stability of the particles was examined by characterization of fresh and used particles in the batch fluidized bed reactor. The oxygen release capability was largely unchanged while the fuel conversion decreased. The decrease was greater for $CaMn_{0.775}Mg_{0.1}Ti_{0.125}O_{3-\delta}$ than for $CaMn_{0.9}Mg_{0.1}O_{3-\delta}$ as is shown in Figure 3.3.5Figure 3.3.5. In an attempt to explain the decrease in reactivity the particles were examined by X-ray powder diffraction. For $CaMn_{0.775}Mg_{0.1}Ti_{0.125}O_{3-\delta}$ an increase in the marokite peaks, $CaMn_2O_4$, was detected, which could be a possible reason for the reduction in reactivity. The decomposition to marokite should be reversible [64] but further work is needed to verify this.

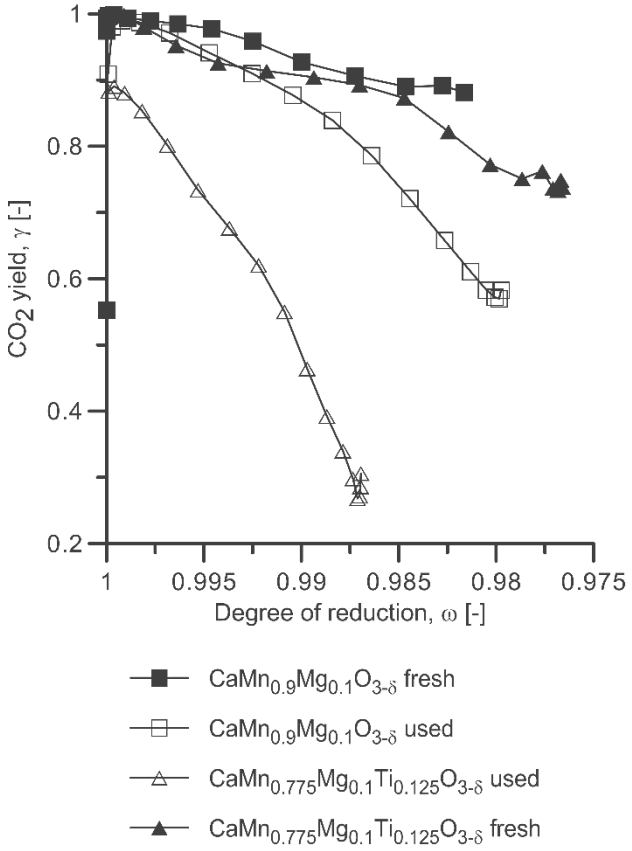

Figure 3.3.5 CO_2 yield as a function of degree of reduction. Results from reduction with methane in fluidized batch reactor. Fresh particles are compared with materials used in the 300 W unit. The experiments were carried out at 950 °C.

3.4 10 kW (Paper IV)

The $CaMn_{0.775}Mg_{0.1}Ti_{0.125}O_{3-\delta}$ as well as the $CaMn_{0.9}Mg_{0.1}O_{3-\delta}$ particles from the 300 W study were selected to be further tested in the 10 kW pilot. Paper IV presents the experimental campaign with $CaMn_{0.775}Mg_{0.1}Ti_{0.125}O_{3-\delta}$ while the work with $CaMn_{0.9}Mg_{0.1}O_{3-\delta}$ is presented in Källén et al. [76]. The experimental campaign with $CaMn_{0.775}Mg_{0.1}Ti_{0.125}O_{3-\delta}$ included 99 h of continuous operation with fuel and substantially longer if all the time with circulation of solids at high temperature would be taken into account. During one warm-up, the fuel reactor and loop seals were fluidized with nitrogen instead of air to be able to examine to oxygen release to inert atmosphere. The oxygen concentration of the gas leaving

the fuel reactor was considerable and similar to the experiment in the 300 W reactor, and is shown as a function of fuel reactor temperature in Figure 3.4.1.

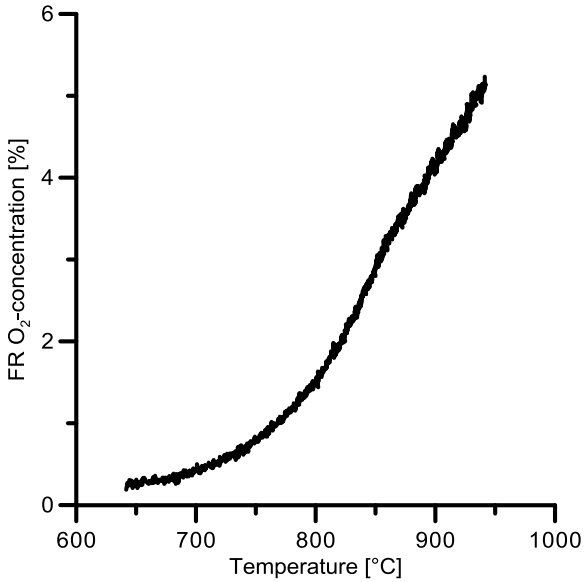

Figure 3.4.1 Oxygen concentration of the gas leaving the fuel reactor during a heat-up period of more than 3 h.

The experimental campaign was carried out over 12 days. The air flow in the air reactor ranged from 160 to 200 L_N/min and the flow of natural gas in the fuel reactor from 4 to 10 L_N/min. The reactor was initially filled with 13 kg particles and in an attempt to increase fuel conversion one additional kg was added after day 7. The elutriation of particles due to unsatisfactory cyclone efficiency was high over the entire campaign. Due to the high elutriation, it was necessary to return particles to the reactor to keep the inventory sufficiently high. As a result the actual particle inventory during operation ranged from 9 to 14 kg. Each time particles were returned from the bag filters to the reactor system a sample of 100 g were taken away and replaced with fresh particles. The samples were sieved to determine the fraction of fines, defined as particles under 45 µm. The mass fraction of fines in each sample is presented in Figure 3.4.2. In three of the samples the amount of fines was too high to measure as the fines clogged the sieve mesh. The high production of fines during the first days of operation could probably be explained by a characteristic of the production method that was used to manufacture the particles which was spray-drying. As particles are formed by spray-drying, some particles come out with so-called satellites which are smaller spheres attached to the larger particles to occur. An example of the small satellites is shown in figure 3.4.3. These are then detached when the particles start to circulate with high gas velocities in the reactor unit and are elutriated as fines. As most satellites are broken off the amount of fines decrease. An analysis of the particle size distribution in Figure 3.4.Figure 3.4.44 also supports this explanation. Some of the particles in the size range 180 – 212 µm would after removal of satellites end up in the 150 – 180 µm range. After day 7 the only fresh particles added to the reactor system was to replenish the samples removed. With this small amounts of fresh particles added the mass fraction of fines was 0 – 0.2 %. The highest mass fraction of fines obtained for this period, 0.2 %, would mean a loss of fines of 0.011 wt%/h, which corresponds to a lifetime above 9 000 h. This is high and could be considered as well above the minimal requirements. Even though the experiment generally went well a reoccurring problem was a stop in circulation due to a build-up of particles in the downward cyclone exit pipe. Fortunately these stops could be dealt with by hitting the upward cyclone exit pipe with a hammer. Each time these stops occurred the CO_2-yield dropped dramatically which is very evident in

Figure 3.4. which shows the dry carbonaceous gases leaving the fuel reactor. The steam has been condensed prior to analysis and the balance is made up of nitrogen used for fluidizing the loop seals.

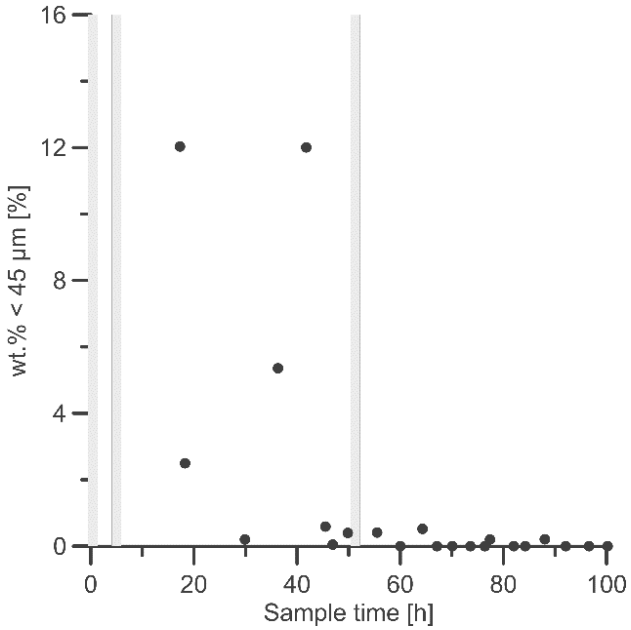

Figure 3.4.2 The mass fraction of particles below 45 µm elutriated from the cyclone. The dots are measured values while the bars represent samples where the fraction of the fines was too high to be accurately measured.

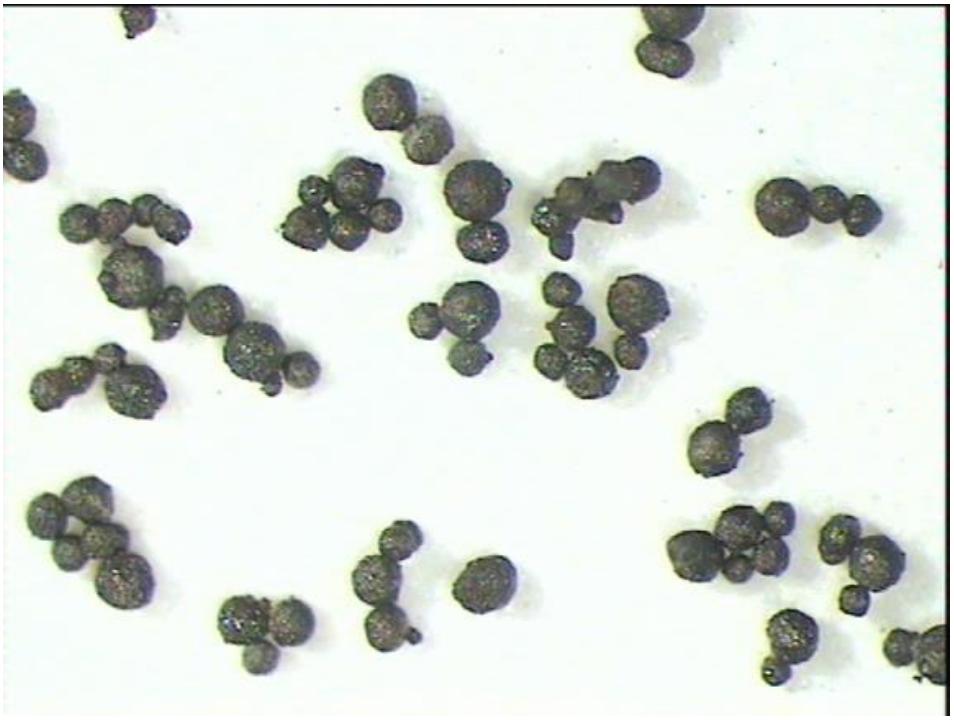

Figur 3.4.3 Light microscope image of unused spray dried particles. Small satellites are attached to some of the larger particles.

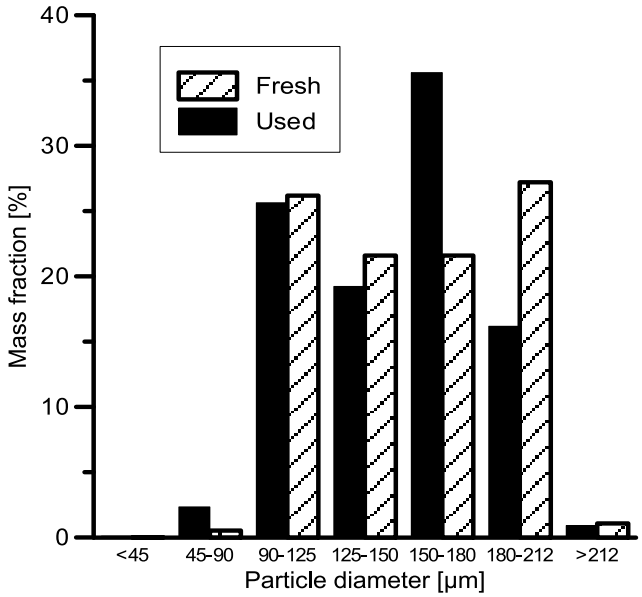

Figure 3.4.4 Particle size distribution of particles before (fresh) and after (used) 99 h of fuel operation.

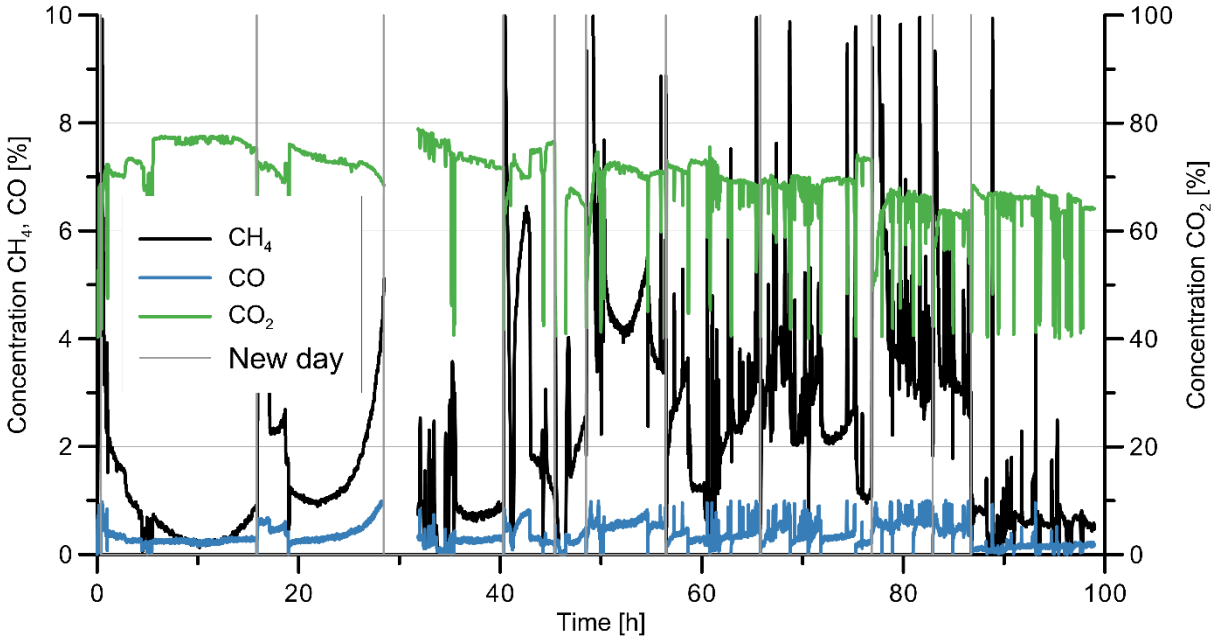

Figure 3.4.5 Compilation of operational data from the run time with natural gas. The grey vertical lines indicate a new day. The first 3.4 h of the fourth day lack data due to a software related problem.

Ten hours of completely uninterrupted operations during day 2 is shown separately in Figure 3.4.66. The average CO_2 yield for this period was over 0.99, which is very high. While all gas flows were held constant during this time of operation it can be seen that the temperature in the fuel reactor slowly decreases. The decrease in temperature can be explained by a decrease in circulation as the oxygen carrier inventory decreases through elutriation of particles. During these ten hours the inventory goes from 13 to 9 kg. During the first five hours the methane concentration of the gas leaving the fuel reactor

slowly decreases, after that the reduced temperature and inventory causes the fuel conversion to slowly decrease.

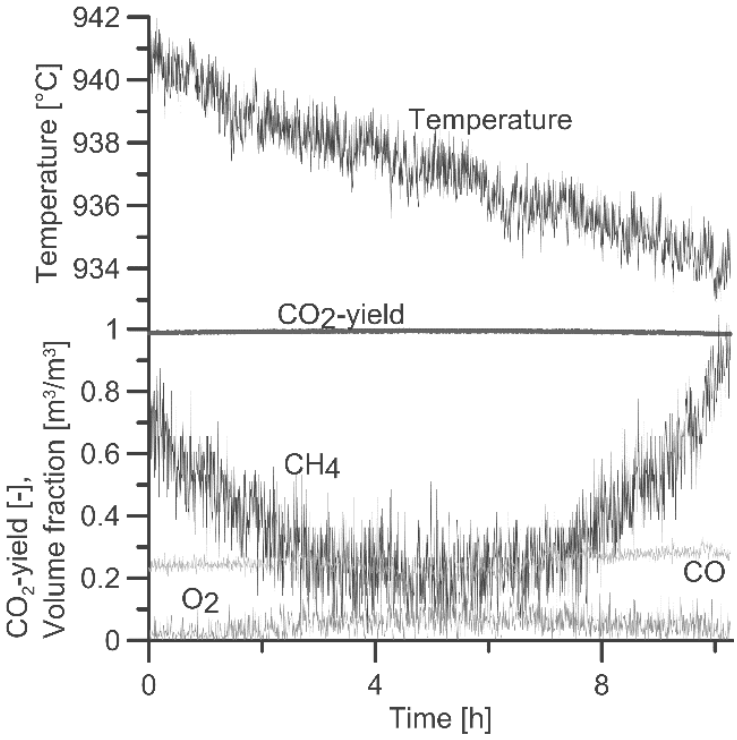

Figure 3.4.6 Fuel reactor temperature, CO_2 yield and fuel reactor concentrations of CO, CH_4 and O_2 for nine hours of operation during Day 2.

A higher CO_2 yield could be reached with a lower fuel flow. That is shown for a specific air flow and temperature in Figure 3.4.Figure 3.4.77. The lower fuel flow also led to a higher air-to-fuel ratio. A high fuel reactor temperature was desired since it beneficially affected the CO_2 yield, the relation is shown in Figure 3.4.Figure 3.4.88 for specific flow settings.

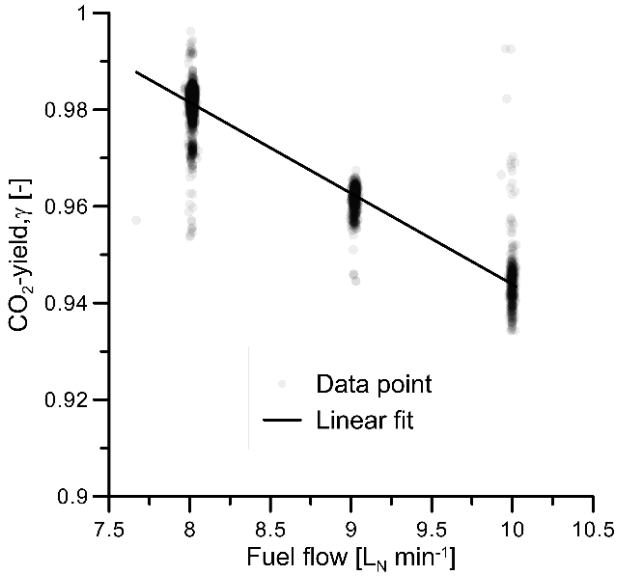

Figure 3.4.7 CO_2 yield as a function of fuel reactor inventory per fuel power at a fuel reactor temperature of approximately 940 °C.

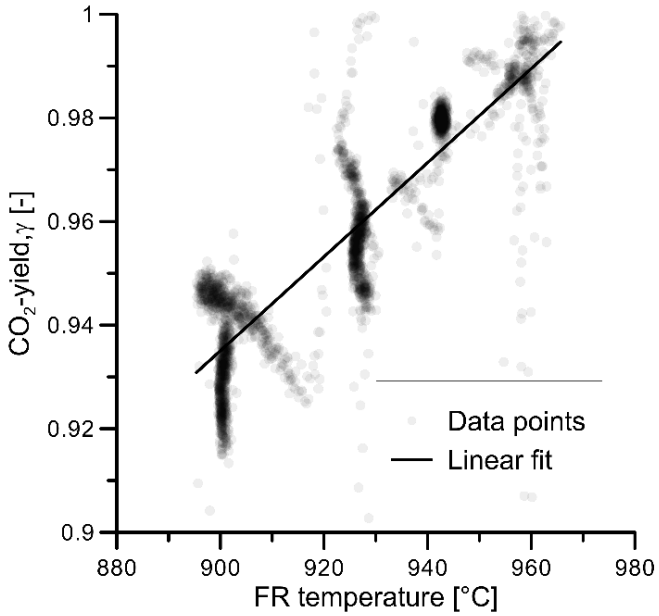

Figure 3.4.8 CO_2 yield as a function of fuel reactor temperature.

In order to determine how the continuous operation had affected the particles reactivity test were carried out in a fluidized batch reactor. These indicated that the ability to release oxygen was unaffected by 99 h of continuous operation. The reactivity with fuel changed only slightly and it was for the better, as is shown in Figure 3.4.Figure 3.4.99. While the effect was minor his contradicts the results from the 300 W-unit, see section 3.3.

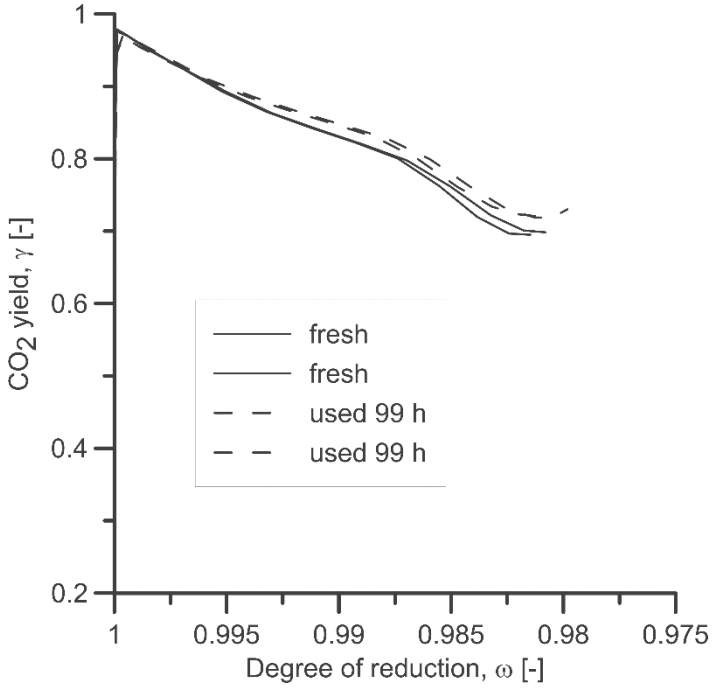

Figure 3.4.9 CO_2 yield as a function of the mass based degree of reduction of oxygen carrier during reaction with methane.

4. DISCUSSION

The main part of this thesis involved the development and step-wise upscaling of oxygen carrier particles based on calcium manganite for chemical-looping combustion of natural gas. The scope of the experimental work went from the use of a small batch reactor via a small continuous reactor to a larger, man-sized, pilot reactor. To a large degree the experiments in the continuous units confirmed the expectations created in the batch experiments. The oxygen release were considerable also in the continuous units and the fuel conversion was complete or close to complete. The attrition of particles stabilized on a low level and in the larger reactor the reactivity with fuel was unchanged. Thus it can be argued that the development scheme outlined in Figure 1.4.2 proved feasible and was successfully implemented, ultimately resulting in the development of synthetic mixed oxide particles with adequate properties for successful operation in a large pilot reactor.

It shall be acknowledged that there were some difficulties encountered during experiments. However, this is to be expected during experimental research and it is not obvious that any of the difficulties were directly caused by the oxygen carriers per se. In the batch reactor there were some occasional fluidization disturbances, but that was not unexpected during experiments using to low fluidization gas velocity and/or to very high temperature. The reason for using such harsh process parameters was that the testing scheme originally was developed for other materials, but was kept the same to facilitate comparison between materials. Also the use of harsh parameters increase the likelihood to identify deficient materials. If a material is sufficiently robust to be operated at very harsh experimental conditions it seems likely to be feasible in practice. If all materials had worked perfectly all the time then we clearly would have tested them at too benign conditions. It would also have made it impossible to distinguish between promising and dubious materials.

The experiments in the 300 W unit went surprisingly well, aside from the problem with particles leakage that occurred but were unrelated to the oxygen carrier material.

Some practical difficulties was experienced during operation of the largest pilot unit. Basically, the 10 kW unit was originally designed for particles with much higher density than the ones used in this work. In fact, the Ni-based particles for which it was designed had more than twice as high density. This has several consequences. As the fuel reactor is a bubbling bed with fixed inventory based on volume, the fuel reactor inventory based on mass were much less. This limited the fuel power input if high fuel conversion was desired. The calcium manganite also have a comparatively small R_O which resulted in the need for a higher oxygen carrier circulation. The high circulation was what caused most difficulties as the upper loop seal and the cyclone repeatedly would overflow and stop circulation. A final factor that was greatly affected by the low particle density was cyclone efficiency. While earlier experiments with Ni-based particles could be operated around the clock with only minor elutriation of solids to the filters, the use of particles with much lower density resulted in poor cyclone efficiency and significant loss of solids as function of time, as has been described above. It seems very likely that a reactor system designed specifically for calcium manganite materials would have provided significantly higher performance on all levels.

One final peculiarity that should be mentioned is that while the fuel reactivity, as measured in batch reactor, for $CaMn_{0.775}Mg_{0.1}Ti_{0.125}O_{3-\delta}$ was unchanged after 99 h in the 10 kW unit it decreased somewhat after 40 h in the 300 W unit. This can be compared with $CaMn_{0.9}Mg_{0.1}O_{3-\delta}$ which reactivity somewhat decreased both in the 300 W unit and after Källens [76] experiment the 10 kW reactor unit. The reason for those deviations are not clear. Efforts undertaken after the finishing of the work presented in this thesis has shown that the influence on calcination/sintering conditions for calcium manganite materials is very significant and affects parameters such as reactivity, density and resistance to attrition. It may be that the addition of elements such as Mg and Ti to the perovskite structure is less important than originally anticipated, while the effect of calcination/sintering is more important. This issue is outside the scope of this thesis though.

5. CONCLUSIONS

The main conclusions from the work presented in this thesis are:

- The temperature change during fuel reduction in the small fluidized bed reactor can be used to determine oxygen carrier reduction enthalpy. This was used to determine that the reaction enthalpy for ilmenite was between that of $FeTiO_3/Fe_2TiO_5$ (445 kJ (mol O_2)$^{-1}$) and Fe_2O_3/Fe_3O_4 (480 kJ (mol O_2)$^{-1}$). Values of 453, 468 and 469 kJ (mol O_2)$^{-1}$ was obtained for synthetic, raw and previously used ilmenite respectively.
- Oxygen carriers based on $CaMn_{1-x}M_xO_{3-\delta}$ with M = Ti, Fe or Mg and x: 0.05-0.25 works well in a small batch reactor. Significant oxygen release as well as high reactivity with syngas and methane were obtained. Calcination temperature had a strong impact on particle crushing strength. 1300 °C for 4 h was enough for satisfactory strength while 1100 or 1200 °C were not.
- In experiments in continuously operating pilot units it was possible to reach complete conversion of natural gas using oxygen carrier based on $CaMn_{1-x}M_xO_{3-\delta}$. This is not possible to achieve with Ni-based oxygen carriers, which previously were the state-of-the-art for CLC of natural gas. Further, these materials showed low rate of attrition, even when used for up to 99 h of operation with fuel in a 10 kW pilot unit utilizing high gas velocities and cyclone. Evaluation of oxygen carrier particles post experiments showed that reactivity was unchanged. After considerable initial attrition of particles the attrition stabilized on a very low level, corresponding to a lifetime of over 9 000 h.

5.1 Epilogue

After having established $CaMnO_{3-\delta}$ based oxygen carriers feasible and highly interesting for chemical-looping combustion application, next step in the development was deemed to be further scale-up of production to industrially relevant volumes and the use of raw materials available in large quantities and at low cost, rather than fine chemicals. Pour et al. manufactured $CaMnO_{3-\delta}$ based oxygen carriers using a manganese ores in a study 2013 [83]. Similar work was made by Mattisson et al. [84]. In the EU-project SUCCESS, a project that followed and built upon the results of the INNOCUOUS project, the main goal was the scale up calcium manganite oxygen carrier production to a batch of >1 ton. This effort was largely performed according to the developing scheme in Figure 1.4.2. Two papers by Jing et al. [85, 86] covers part of the work from the initial steps while Hallberg et al. [87] presents part of the work done in step 5.

6. REFERENCES

1. Arrhenius, S., *On the influence of carbonic acid in the air upon the temperature of the ground.* Philos Mag, 1886. **41**: p. 237-277.
2. Bindoff, N.L., P.A. Stott, K.M. AchutaRao, M.R. Allen, N. Gillett, D. Gutzler, K. Hansingo, G. Hegerl, Y. Hu, S. Jain, I.I. Mokhov, J. Overland, J. Perlwitz, R. Sebbari, and X. Zhang, *Detection and Attribution of Climate Change: from Global to Regional*, in *Climate Change 2013: The Physical Science Basis. Contribution of Working Group I to the Fifth Assessment Report of the Intergovernmental Panel on Climate Change*, T.F. Stocker, et al., Editors. 2013, Cambridge University Press: Cambridge, United Kingdom and New York, NY, USA. p. 867–952.
3. United Nations / Framework Convention on Climate Change (2015) Adoption of the Paris Agreement and P.U.N. 21st Conference of the Parties.
4. Stéphenne, K., *Start-up of World's First Commercial Post-combustion Coal Fired CCS Project: Contribution of Shell Cansolv to SaskPower Boundary Dam ICCS Project.* Energy Procedia, 2014. **63**: p. 6106-6110.
5. IPPC, I.P.o.C.C., *Carbon Dioxide Capture and Storage*, www.ipcc.ch, Editor. 2005.
6. Ishida, M. and H. Jin, *A new advanced power-generation system using chemical-looping combustion.* Energy, 1994. **19**(4): p. 415-422.
7. Ströhle, J., M. Orth, and B. Epple, *Design and operation of a 1 MWth chemical looping plant.* Applied Energy, 2014. **113**: p. 1490-1495.
8. Vilches, T.B., F. Lind, M. Rydén, and H. Thunman, *Experience of more than 1000 h of operation with oxygen carriers and solid biomass at large scale.* Applied Energy, 2017. **190**: p. 1174-1183.
9. Hossain, M.M. and H.I. de Lasa, *Chemical-looping combustion(CLC) for inherent CO_2 separation – A review.* Chemical Engineering Science, 2008. **63**: p. 4433-4451.
10. Fang, H., L. Haibin, and Z. Zengli, *Advancements in Development of Chemical-Looping Combustion: A Review.* International Journal of Chemical Engineering, 2009. **2009**: p. 16.
11. Adanez, J., A. Abad, F. Garcia-Labiano, P. Gayan, and L.F. De Diego, *Progress in chemical-looping combustion and reforming technologies.* Progress in Energy and Combustion Science, 2012. **38**(2): p. 215-282.
12. Fan, L.-S. and F. Li, *Chemical Looping Technology and Its Fossil Energy Conversion Applications.* Industrial & Engineering Chemistry Research, 2010. **49**(21): p. 10200-10211.
13. Moghtaderi, B., *Review of the Recent Chemical Looping Process Developments for Novel Energy and Fuel Applications.* Energy & Fuels, 2012. **26**(1): p. 15-40.
14. Lyngfelt, A., *Chemical-looping combustion of solid fuels – Status of development.* Applied Energy, 2014. **113**: p. 1869-1873.
15. Fan, L.-S., *Chemical Looping Systems for Fossil Energy Conversion*. 2010, Hoboken, New Jersey: John Wiley & Sons, Inc.
16. *Calcium and chemical looping technology for power generation and carbon dioxide (CO2) capture*. 2015: Woodland Publishing.
17. Noorman, S., M. van Sint Annaland, and Kuipers, *Packed Bed Reactor Technology for Chemical-Looping Combustion.* Industrial & Engineering Chemistry Research, 2007. **46**(12): p. 4212-4220.
18. Hamers, H.P., F. Gallucci, P.D. Cobden, E. Kimball, and M. van Sint Annaland, *A novel reactor configuration for packed bed chemical-looping combustion of syngas.* International Journal of Greenhouse Gas Control, 2013. **16**: p. 1-12.

19. Spallina, V., M.C. Romano, P. Chiesa, F. Gallucci, M. van Sint Annaland, and G. Lozza, *Integration of coal gasification and packed bed CLC for high efficiency and near-zero emission power generation.* International Journal of Greenhouse Gas Control, 2014. **27**: p. 28-41.
20. Gallucci, F., H.P. Hamers, M. van Zanten, and M. van Sint Annaland, *Experimental demonstration of chemical-looping combustion of syngas in packed bed reactors with ilmenite.* Chemical Engineering Journal, 2015. **274**: p. 156-168.
21. Fernández, J.R. and J.M. Alarcón, *Chemical looping combustion process in fixed-bed reactors using ilmenite as oxygen carrier: Conceptual design and operation strategy.* Chemical Engineering Journal, 2015. **264**: p. 797-806.
22. Mattisson, T., A. Lyngfelt, and H. Leion, *Chemical-looping with oxygen uncoupling for combustion of solid fuels.* International Journal of Greenhouse Gas Control, 2009. **3**(1): p. 11-19.
23. Mayer, K., S. Penthor, T. Pröll, and H. Hofbauer, *The different demands of oxygen carriers on the reactor system of a CLC plant - Results of oxygen carrier testing in a 120 kWth pilot plant.* Applied Energy, 2015. **157**: p. 323-329.
24. Abad, A., P. Gayán, L.F. de Diego, F. García-Labiano, J. Adánez, K. Mayer, and S. Penthor. *Modelling a CLC process improved by CLOU and validation in a 120 kw unit*. in *CFB-11: Proceedings of the 11th International Conference on Fluidized Bed Technology*. 2014.
25. Rydén, M. and A. Lyngfelt, *Hydrogen and power production with integrated carbon dioxide capture by chemical-looping reforming*, in *Greenhouse Gas Control Technologies 7*. 2005, Elsevier Science Ltd: Oxford. p. 125-134.
26. Jerndal, E., T. Mattisson, and A. Lyngfelt, *Investigation of Different NiO/NiAl2O4 Particles as Oxygen Carriers for Chemical-Looping Combustion.* Energy & Fuels, 2009. **23**(2): p. 665-676.
27. Linderholm, C., T. Mattisson, and A. Lyngfelt, *Long-term integrity testing of spray-dried particles in a 10-kW chemical-looping combustor using natural gas as fuel.* Fuel, 2009. **88**(11): p. 2083-2096.
28. Bolhàr-Nordenkampf, J., T. Pröll, P. Kolbitsch, and H. Hofbauer. *Performance of a NiO-based oxygen carrier for chemical looping combustion and reforming in a 120 kW unit*. in *Energy Procedia*. 2009.
29. Adánez, J., C. Dueso, L.F.D. Diego, F. García-Labiano, P. Gayán, and A. Abad, *Methane combustion in a 500 Wth chemical-looping combustion system using an impregnated ni-based oxygen carrier.* Energy and Fuels, 2009. **23**(1): p. 130-142.
30. Abad, A., I. Adánez-Rubio, P. Gayán, F. García-Labiano, L.F. de Diego, and J. Adánez, *Demonstration of chemical-looping with oxygen uncoupling (CLOU) process in a 1.5kW th continuously operating unit using a Cu-based oxygen-carrier.* International Journal of Greenhouse Gas Control, 2012. **6**: p. 189-200.
31. Mei, D., H. Zhao, Z. Ma, and C. Zheng, *Using the Sol–Gel-Derived CuO/CuAl2O4 Oxygen Carrier in Chemical Looping with Oxygen Uncoupling for Three Typical Coals.* Energy & Fuels, 2013. **27**(5): p. 2723-2731.
32. de Diego, L.F., F. Garcia-Labiano, P. Gayan, J. Celaya, J.M. Palacios, and J. Adanez, *Operation of a 10kWth chemical-looping combustor during 200h with a CuO-Al_2O_3 oxygen carrier.* Fuel, 2007. **86**(7-8): p. 1036-1045.
33. Adánez-Rubio, I., P. Gayán, A. Abad, L.F. De Diego, F. García-Labiano, and J. Adánez, *Evaluation of a spray-dried CuO/MgAl 2O 4 oxygen carrier for the chemical looping with oxygen uncoupling process.* Energy and Fuels, 2012. **26**(5): p. 3069-3081.

34. Rydén, M., D. Jing, M. Källén, H. Leion, A. Lyngfelt, and T. Mattisson, *CuO-based oxygen-carrier particles for chemical-looping with oxygen uncoupling - Experiments in batch reactor and in continuous operation.* Industrial and Engineering Chemistry Research, 2014. **53**(15): p. 6255-6267.
35. Penthor, S., F. Zerobin, K. Mayer, T. Pröll, and H. Hofbauer, *Investigation of the performance of a copper based oxygen carrier for chemical looping combustion in a 120kW pilot plant for gaseous fuels.* Applied Energy, 2015. **145**: p. 52-59.
36. Ku, Y., S.-H. Shiu, Y.-C. Liu, H.-C. Wu, Y.-L. Kuo, and H.-Y. Lee, *Liquid sintering behavior of Cu-based oxygen carriers for chemical looping process.* Catalysis Communications, 2017. **92**: p. 70-74.
37. Abad, A., T. Mattisson, A. Lyngfelt, and M. Johansson, *The use of iron oxide as oxygen carrier in a chemical-looping reactor.* Fuel, 2007. **86**(7-8): p. 1021-1035.
38. Johansson, M., T. Mattisson, and A. Lyngfelt, *Investigation of Fe_2O_3 with $MgAl_2O_4$ for Chemical-Looping Combustion.* Industrial & Engineering Chemistry Research, 2004. **43**(22): p. 6978-6987.
39. Zafar, Q., A. Abad, T. Mattisson, B. Gevert, and M. Strand, *Reduction and oxidation kinetics of Mn3O4/Mg–ZrO2 oxygen carrier particles for chemical-looping combustion* Chemical Engineering Science, 2007. **62**(23): p. 6556-6567
40. Jerndal, E., T. Mattisson, and A. Lyngfelt, *Thermal analysis of chemical-looping combustion.* Chemical Engineering Research and Design, 2006. **84**(A9): p. 795-806.
41. Linderholm, C., A. Abad, T. Mattisson, and A. Lyngfelt, *160 hours of chemical-looping combustion in a 10 kW reactor system with a NiO-based oxygen carrier.* International Journal of Greenhouse Gas Control, 2008. **2**(4): p. 520-530.
42. Azimi, G., H. Leion, M. Rydén, T. Mattisson, and A. Lyngfelt, *Investigation of Different Mn–Fe Oxides as Oxygen Carrier for Chemical-Looping with Oxygen Uncoupling (CLOU).* Energy & Fuels, 2013. **27**(1): p. 367-377.
43. Azimi, G., T. Mattisson, H. Leion, M. Rydén, and A. Lyngfelt, *Comprehensive study of Mn–Fe–Al oxygen-carriers for chemical-looping with oxygen uncoupling (CLOU).* International Journal of Greenhouse Gas Control, 2015. **34**: p. 12-24.
44. Azimi, G., H. Leion, T. Mattisson, M. Rydén, F. Snijkers, and A. Lyngfelt, *Mn–Fe Oxides with Support of MgAl2O4, CeO2, ZrO2 and Y2O3–ZrO2 for Chemical-Looping Combustion and Chemical-Looping with Oxygen Uncoupling.* Industrial & Engineering Chemistry Research, 2014. **53**(25): p. 10358-10365.
45. Rydén, M., A. Lyngfelt, and T. Mattisson, *Combined manganese/iron oxides as oxygen carrier for chemical looping combustion with oxygen uncoupling (CLOU) in a circulating fluidized bed reactor system.* Energy Procedia, 2011. **4**: p. 341-348.
46. Haider, S.K., G. Azimi, L. Duan, E.J. Anthony, K. Patchigolla, J.E. Oakey, H. Leion, T. Mattisson, and A. Lyngfelt, *Enhancing properties of iron and manganese ores as oxygen carriers for chemical looping processes by dry impregnation.* Applied Energy, 2016. **163**: p. 41-50.
47. Shafiefarhood, A., A. Stewart, and F. Li, *Iron-containing mixed-oxide composites as oxygen carriers for Chemical Looping with Oxygen Uncoupling (CLOU).* Fuel, 2015. **139**: p. 1-10.
48. Shulman, A., E. Cleverstam, T. Mattisson, and A. Lyngfelt, *Manganese/Iron, Manganese/Nickel, and Manganese/Silicon Oxides Used in Chemical-Looping With Oxygen Uncoupling (CLOU) for Combustion of Methane.* Energy & Fuels, 2009. **23**(10): p. 5269-5275.

49. Bhavsar, S., B. Tackett, and G. Veser, *Evaluation of iron- and manganese-based mono- and mixed-metallic oxygen carriers for chemical looping combustion.* Fuel, 2014. **136**: p. 268-279.
50. Larring, Y., C. Braley, M. Pishahang, K.A. Andreassen, and R. Bredesen, *Evaluation of a Mixed Fe–Mn Oxide System for Chemical Looping Combustion.* Energy & Fuels, 2015. **29**(5): p. 3438-3445.
51. Mattisson, T., D. Jing, A. Lyngfelt, and M. Rydén, *Experimental investigation of binary and ternary combined manganese oxides for chemical-looping with oxygen uncoupling (CLOU).* Fuel, 2016. **164**: p. 228-236.
52. Källén, M., P. Hallberg, M. Rydén, T. Mattisson, and A. Lyngfelt, *Combined oxides of iron, manganese and silica as oxygen carriers for chemical-looping combustion.* Fuel Processing Technology, 2014. **124**: p. 87-96.
53. Källén, M., M. Rydén, A. Lyngfelt, and T. Mattisson, *Chemical-looping combustion using combined iron/manganese/silicon oxygen carriers.* Applied Energy, 2015. **157**: p. 330-337.
54. Källén, M., M. Rydén, T. Mattisson, and A. Lyngfelt, *Operation with Combined Oxides of Manganese and Silica as Oxygen Carriers in a 300 Wth Chemical-looping Combustion Unit.* Energy Procedia, 2014. **63**: p. 131-139.
55. Shulman, A., E. Cleverstam, T. Mattisson, and A. Lyngfelt, *Chemical – Looping with oxygen uncoupling using Mn/Mg-based oxygen carriers – Oxygen release and reactivity with methane.* Fuel, 2011. **90**(3): p. 941-950.
56. Leion, H., Y. Larring, E. Bakken, R. Bredesen, T. Mattisson, and A. Lyngfelt, *The use of $CaMn_{0.875}Ti_{0.125}O_3$ as oxygen carrier in Chemical-Looping with Oxygen Uncoupling (CLOU).* Energy & Fuels, 2009. **23**: p. 5276-5283.
57. Rydén, M., A. Lyngfelt, and T. Mattisson, *CaMn0.875Ti0.125O3 as oxygen carrier for chemical-looping combustion with oxygen uncoupling (CLOU)—Experiments in a continuously operating fluidized-bed reactor system.* International Journal of Greenhouse Gas Control, 2011. **5**(2): p. 356-366.
58. Fossdal, A., E. Bakken, B.A. Øye, C. Schøning, I. Kaus, T. Mokkelbost, and Y. Larring, *Study of inexpensive oxygen carriers for chemical looping combustion.* International Journal of Greenhouse Gas Control, 2011. **5**(3): p. 483-488.
59. Leonidova, E.I., I.A. Leonidov, M.V. Patrakeev, and V.L. Kozhevnikov, *Oxygen non-stoichiometry, high-temperature properties, and phase diagram of CaMnO3–δ.* Journal of Solid State Electrochemistry, 2011. **15**(5): p. 1071-1075.
60. Li, C., K.C.K. Soh, and P. Wu, *Formability of ABO3 perovskites.* Journal of Alloys and Compounds, 2004. **372**(1–2): p. 40-48.
61. Rørmark, L., A.B. Mørch, K. Wiik, S. Stølen, and T. Grande, *Enthalpies of oxidation of CaMnO3-δ, Ca2MnO4-δ and SrMnO3-δ - Deduced redox properties.* Chemistry of Materials, 2001. **13**(11): p. 4005-4013.
62. Abad, A., F. García-Labiano, P. Gayán, L.F. de Diego, and J. Adánez, *Redox kinetics of CaMg0.1Ti0.125Mn0.775O2.9–δ for Chemical Looping Combustion (CLC) and Chemical Looping with Oxygen Uncoupling (CLOU).* Chemical Engineering Journal, 2015. **269**: p. 67-81.
63. Sarshar, Z., Z. Sun, D. Zhao, and S. Kaliaguine, *Development of sinter-resistant core-shell LaMn xFe 1- xO 3@mSiO 2 oxygen carriers for chemical looping combustion.* Energy and Fuels, 2012. **26**(5): p. 3091-3102.

64. Bakken, E., T. Norby, and S. Stølen, *Nonstoichiometry and reductive decomposition of $CaMnO_{3-\delta}$* Solid State Ionics, 2004. **176**(1-2): p. 217-223
65. Galinsky, N., M. Sendi, L. Bowers, and F. Li, *CaMn1−xBxO3−δ (B = Al, V, Fe, Co, and Ni) perovskite based oxygen carriers for chemical looping with oxygen uncoupling (CLOU).* Applied Energy, 2016. **174**: p. 80-87.
66. Galinsky, N., A. Mishra, J. Zhang, and F. Li, *Ca1−xAxMnO3 (A = Sr and Ba) perovskite based oxygen carriers for chemical looping with oxygen uncoupling (CLOU).* Applied Energy, 2015. **157**: p. 358-367.
67. Arjmand, M., A. Hedayati, A.-M. Azad, H. Leion, M. Rydén, and T. Mattisson, *CaxLa1−xMn1−yMyO3−δ (M = Mg, Ti, Fe, or Cu) as Oxygen Carriers for Chemical-Looping with Oxygen Uncoupling (CLOU).* Energy & Fuels, 2013. **27**(8): p. 4097-4107.
68. Arjmand, M., R.F. Kooiman, M. Rydén, H. Leion, T. Mattisson, and A. Lyngfelt, *Sulfur Tolerance of CaxMn1−yMyO3−δ (M = Mg, Ti) Perovskite-Type Oxygen Carriers in Chemical-Looping with Oxygen Uncoupling (CLOU).* Energy & Fuels, 2014. **28**(2): p. 1312-1324.
69. Cabello, A., A. Abad, P. Gayán, L.F. de Diego, F. García-Labiano, and J. Adánez, *Effect of Operating Conditions and H2S Presence on the Performance of CaMg0.1Mn0.9O3−δ Perovskite Material in Chemical Looping Combustion (CLC).* Energy & Fuels, 2014. **28**(2): p. 1262-1274.
70. Schmitz, M., C. Linderholm, and A. Lyngfelt, *Chemical Looping Combustion of Sulphurous Solid Fuels Using Spray-dried Calcium Manganate Particles as Oxygen Carrier.* Energy Procedia, 2014. **63**: p. 140-152.
71. Schmitz, M. and C.J. Linderholm, *Performance of calcium manganate as oxygen carrier in chemical looping combustion of biochar in a 10 kW pilot.* Applied Energy, 2016. **169**: p. 729-737.
72. Moldenhauer, P., M. Rydén, T. Mattisson, A. Hoteit, A. Jamal, and A. Lyngfelt, *Chemical-Looping Combustion with Fuel Oil in a 10 kW Pilot Plant.* Energy & Fuels, 2014. **28**(9): p. 5978-5987.
73. Moldenhauer, P., M. Rydén, T. Mattisson, A. Jamal, and A. Lyngfelt, *Chemical-looping combustion with heavy liquid fuels in a 10 kW pilot plant.* Fuel Processing Technology, 2017. **156**: p. 124-137.
74. Cuadrat, A., A. Abad, J. Adánez, L.F. de Diego, F. García-Labiano, and P. Gayán, *Behavior of ilmenite as oxygen carrier in chemical-looping combustion.* Fuel Processing Technology, 2012. **94**(1): p. 101-112.
75. Jing, D., T. Mattisson, M. Ryden, P. Hallberg, A. Hedayati, J. Van Noyen, F. Snijkers, and A. Lyngfelt, *Innovative Oxygen Carrier Materials for Chemical-Looping Combustion.* Energy Procedia, 2013. **37**(0): p. 645-653.
76. Källén, M., M. Rydén, C. Dueso, T. Mattisson, and A. Lyngfelt, *CaMn0.9Mg0.1O3-δ as Oxygen Carrier in a Gas-Fired 10 kWthChemical-Looping Combustion Unit.* Industrial & Engineering Chemistry Research, 2013. **52**(21): p. 6923-6932.
77. Sundqvist, S., H. Leion, M. Rydén, A. Lyngfelt, and T. Mattisson, *CaMn0.875Ti0.125O3−δ as an Oxygen Carrier for Chemical-Looping with Oxygen Uncoupling (CLOU)—Solid-Fuel Testing and Sulfur Interaction.* Energy Technology, 2013. **1**(5-6): p. 338-344.
78. Jing, D., T. Mattisson, H. Leion, Ryd, #xe9, M. n, and A. Lyngfelt, *Examination of Perovskite Structure CaMnO3-δ with MgO Addition as Oxygen Carrier for Chemical Looping with Oxygen Uncoupling Using Methane and Syngas.* International Journal of Chemical Engineering, 2013. **2013**: p. 16.

79. Jing, D., M. Arjmand, T. Mattisson, M. Rydén, F. Snijkers, H. Leion, and A. Lyngfelt, *Examination of oxygen uncoupling behaviour and reactivity towards methane for manganese silicate oxygen carriers in chemical-looping combustion.* International Journal of Greenhouse Gas Control, 2014. 29: p. 70-81.
80. Rydén, M., M. Källén, D. Jing, A. Hedayati, T. Mattisson, and A. Lyngfelt, *(Fe1-xMnx)TiyO3 based Oxygen Carriers for Chemical-looping Combustion and Chemical-looping with Oxygen Uncoupling.* Energy Procedia, 2014. 51: p. 85-98.
81. Mattisson, T., J. Adánez, K. Mayer, F. Snijkers, G. Williams, E. Wesker, O. Bertsch, and A. Lyngfelt, *Innovative Oxygen Carriers Uplifting Chemical-looping Combustion.* Energy Procedia, 2014. 63: p. 113-130.
82. Rydén, M., P. Moldenhauer, S. Lindqvist, T. Mattisson, and A. Lyngfelt, *Measuring attrition resistance of oxygen carrier particles for chemical looping combustion with a customized jet cup.* Powder Technology, 2014. 256: p. 75-86.
83. Pour, N.M., G. Azimi, H. Leion, M. Rydén, and A. Lyngfelt, *Production and examination of oxygen-carrier materials based on manganese ores and Ca(OH)2 in chemical looping with oxygen uncoupling.* AIChE Journal, 2014. 60(2): p. 645-656.
84. Mattisson, T., C. Linderholm, E. Jerndal, and A. Lyngfelt, *Enhanced performance of manganese ore as oxygen carrier for chemical-looping with oxygen uncoupling (CLOU) by combination with Ca(OH)2 through spray-drying.* Journal of Environmental Chemical Engineering, 2016. 4(4, Part A): p. 3707-3717.
85. Jing, D., M. Jacobs, P. Hallberg, A. Lyngfelt, and T. Mattisson, *Development of CaMn0.775Mg0.1Ti0.125O3-δ oxygen carriers produced from different Mn and Ti sources.* Materials & Design, 2016. 89: p. 527-542.
86. Jing, D., F. Snijkers, P. Hallberg, H. Leion, T. Mattisson, and A. Lyngfelt, *Effect of Production Parameters on the Spray-Dried Calcium Manganite Oxygen Carriers for Chemical-Looping Combustion.* Energy & Fuels, 2016. 30(4): p. 3257-3268.
87. Hallberg, P., M. Rydén, T. Mattisson, and A. Lyngfelt, *CaMnO3-δ Made from Low Cost Material Examined as Oxygen Carrier in Chemical-looping Combustion.* Energy Procedia, 2014. 63: p. 80-86.